

UNIVERSIDADE DE LISBOA
FACULDADE DE CIÊNCIAS
DEPARTAMENTO DE BIOLOGIA VEGETAL



Study of the Photosynthetic Response to
Drought Stress in AOX Mutants of
Arabidopsis thaliana

João Lucas Fidalgo Oliveira Coito

Mestrado em Biologia Celular e Biotecnologia

2009

UNIVERSIDADE DE LISBOA
FACULDADE DE CIÊNCIAS
DEPARTAMENTO DE BIOLOGIA VEGETAL



Study of the Photosynthetic Response to
Drought Stress in AOX Mutants of
Arabidopsis thaliana

João Lucas Fidalgo Oliveira Coito

Dissertação orientada pelo Prof. Doutor Jorge Marques da Silva e pela Prof.
Doutora Ana Rita Matos

Mestrado em Biologia Celular e Biotecnologia

2009

“The important thing is not to stop questioning. Curiosity has its own reason for existing. One cannot help but be in awe when he contemplates the mysteries of eternity, of life, of the marvelous structure of reality. It is enough if one tries merely to comprehend a little of this mystery every day. Never lose a holy curiosity.”

Albert Einstein (1879 – 1955)

Acknowledgements

This work was conducted in the former Centro de Engenharia Biológica, now Center for Biodiversity, Functional & Integrative Genomics, in Departamento de Biologia Vegetal, Faculdade de Ciências da Universidade de Lisboa under the supervision of Prof. Doutor Jorge Marques da Silva and Prof. Doutora Ana Rita Matos.

To Prof. Doutor Jorge Marques da Silva and Prof. Doutora Ana Rita Matos, I would like to thank for agreeing to be my advisors and for supporting my work at the center.

I also want to thank Prof. Doutor Jorge Marques da Silva for all the help given in understanding plants water relations and chlorophyll fluorescence as well as an important lesson regarding statistic analysis of the data and overall data organization.

To Prof. Doutora Ana Rita Matos I would like to thank all the help and lessons in molecular biology as well as advices in how to make this work more complete. These were lessons that will stay with me in my future as a biologist.

To Prof. Doutora Anabela Bernardes da Silva I would like to thank all the support especially the help regarding calculations and analysis of photosynthetic parameters as well as all the support I've receive throughout the passing year.

To all the rest of the team, Prof. Doutora Adalcina Casimiro, Prof. Doutora Maria Celeste Arrabaça and Prof. Doutor João Daniel Arrabaça, I would like to thank for all the sympathy with which they receive me in the laboratory.

I would also like to thank D. Manuela Lucas for all the support in the lab and all the life lessons she kindly taught me.

To the almost Doctor Ricardo Carvalho, Dave Pinxteren, and Célia Lima for the company they provide me this whole year working the lab, I am grateful. Although probably I shouldn't say this, it's nice to have someone to talk about, either work or just normal life situations.

To my family and friends, for all reasons I cannot possibly describe here, without whom this work would not have been possible, I am deeply grateful.

Thank you all.

Abstract

Plant metabolism is modulated in a very dynamic way, being dependent on environmental factors.

The integration between photosynthesis and respiration is a key-aspect of metabolic regulation. Photorespiration may play an important role on the integration of chloroplastidial and mitochondrial metabolism, as photorespiratory NADH might be oxidized in the respiratory chain by internal type II NAD(P)H dehydrogenases and alternative oxidase (AOX).

This work aims to test the role of AOX in the mitochondrial redox potential dissipation that occurs during photosynthesis and photorespiration under water stress. The hypothesis is that AOX plays an important role and its lower activity will reflect itself in photosynthesis and photorespiration. For that, wild type (Col-0) *Arabidopsis* and *AOX1a* transgenic *Arabidopsis* (AS-AOX1a) were used.

No morphological differences were found between the two lines of plants under control or stress conditions. However, higher Specific Leaf Area and stomatal conductance were observed in the transgenic plants under mild stress, whereas their water potential was lower. A more pronounced decrease in photorespiration with drought in AS-AOX1a plants was also detected, having reflected itself in the photorespiration / photosynthesis ratio, which was lower in these plants. The observed decrease in ETR and qP might indicate that the quinone pool had become more reduced in both lines of plants, but the curvilinear decrease on AS-AOX1a contrasts with the linear trend in Col-0, suggesting differences on the dynamics of stress sensing and response. A very highly significant increase of NPQ under stress was found on AS-AOX1a plants, in contrast with Col-0 plants, where the increase was much less sensible, suggesting an increase on the activity of alternative energy dissipating mechanisms on the former, which is in accordance with lower photorespiration rates. Lower amounts of *GDC-P1* and *UCP1* transcripts were detected in AS-AOX1a, which is also in agreement with the lower photorespiration rate in these plants. In contrast, the *SHMT* transcripts increased with drought stress in both plant lines and were higher in AS-AOX1a

All together the results suggest that the AS plants AS being impaired in the expression of AOX1a display alterations in the photorespiratory process.

Keywords: Photorespiration; Photosynthesis; AS-AOX1a; AOX; Drought stress.

Resumo

A relação entre cloroplastos e mitocôndrias nas plantas é modulada de forma dinâmica, sendo dependente de factores ambientais.

A integração entre fotossíntese e respiração é um aspecto-chave da regulação metabólica. A fotorrespiração pode desempenhar um papel central na integração do metabolismo cloroplastidial com o metabolismo mitocondrial, uma vez que o NADH fotorrespiratório poderá ser oxidado na cadeia respiratória pelas NAD(P)H desidrogenases internas tipo II e pela oxidase alternativa (AOX).

Este trabalho visa testar o papel da AOX na dissipação do potencial redox que se forma na mitocôndria e que ocorre durante a fotossíntese sob stress hídrico. A hipótese é a de que a AOX desempenha um papel importante e a sua reduzida actividade irá reflectir-se tanto na fotossíntese como na fotorrespiração. Para tal, serão usadas *Arabidopsis* selvagens (Col-0) e *Arabidopsis* transgénicas AOX1a (AS-AOX1a).

Não foram encontradas diferenças morfológicas entre as duas linhas de plantas em condições controle ou de stress. No entanto, foi detectada uma maior Área Foliar Específica e condutância estomática nas plantas transgénicas sob stress moderado, enquanto o seu potencial hídrico se revelou mais baixo. Foi ainda detectada uma diminuição mais acentuada da fotorrespiração com o deficit hídrico, em plantas AS-AOX1a, que se reflectiu na razão fotorrespiração / fotossíntese, que foi menor nessas plantas. Observou-se uma diminuição, em stress, de ETR e qP que pode sugerir que nas duas linhas de plantas o “pool” de quinonas se tornou mais reduzido, mas a forma de variação curvilínea em AS-AOX1a e linear em Col-0 sugere diferenças na dinâmica de sinalização e resposta ao stress. O aumento muito significativo de NPQ, em stress, nas plantas AS-AOX1a, em contraste com o aumento pouco expressivo em Col-0, sugere que nas primeiras estão mais activos mecanismos alternativos de dissipação de energia, o que está de acordo com a suas menores taxas respiratórias. Também a menor expressão de *GDC-P1* e *UCP1* detectada nas plantas AS-AOX1a está de acordo com a sua menor taxa fotorrespiratória, ainda que a expressão de *SHMT* tenha aumentado nos dois génotipos em condições de stress e seja superior em AS-AOX1a.

Em conjunto os resultados sugerem que as plantas AS-AOX1a ao serem limitadas na expressão de *AOX1a* apresentam alterações no processo fotorrespiratório.

Palavras-chave: Fotorrespiração; Fotossíntese; AS-AOX1a; AOX; Stress hídrico.

Resumo Alargado

Durante os últimos anos, tem-se observado um interesse crescente no estudo da relação metabólica entre cloroplastos e mitocôndrias. Em folhas iluminadas o metabolismo é modulado de forma muito dinâmica. Em condições de stress as funções de cloroplastos e mitocôndrias são ainda mais estreitamente coordenadas.

A principal função das reacções fotoquímicas é a produção de ATP e de potencial redutor na forma de NADPH, necessários à redução de compostos carbonatados. A cadeia de transporte electrónico na membrana tilacoidal é composta por dois fotossistemas (PSI e PSII) e um complexo proteico que inclui o citocromo b6/f. Os electrões resultantes do desdobramento de moléculas de água dependente da luz são transportados através da cadeia de transporte de electrões com produção de ATP e NADPH. A fixação de dióxido de carbono (CO₂) ocorre no ciclo de Calvin, que condensa uma molécula de CO₂ atmosférico com ribulose-1,5-bisfosfato (RuBP) para produzir duas moléculas de 3-fosfoglicerato, que é mais tarde transformado em ATP e redutores na respiração. A incapacidade de escoar o excesso de energia que ocorre neste processo, em condições ambientais desfavoráveis, pode levar a que ocorra stress oxidativo e consequentemente danos, não só, no aparelho fotossintético, mas também noutras zonas da célula, comprometendo a sua sobrevivência.

Um dos processos de dissipação de energia ocorre através da fotorrespiração. Sob concentrações atmosféricas de CO₂, a competição entre este e o O₂ pelos centros activos da Rubisco faz com que haja actividade oxigenativa, com produção de 2-fosfoglicolato (PGly) que pode ser convertido em glicerato em sucessivas reacções no cloroplasto, peroxissoma e na mitocôndria. Nestas reacções destaca-se o complexo glicina descarboxilase – serina hidroximetil transferase (GDC-SMHT) presente na mitocôndria e que converte glicina (Gly) e NAD⁺ em serina (Ser), NADH, CO₂ e NH⁴⁺. Também nas mitocôndrias existe, além da via fosforilativa (que engloba os complexos I, II, III e IV), várias enzimas pertencentes a uma via não fosforilativa como as NADH desidrogenases internas (NDins) e a oxidase alternativa (AOX), cujas funções fisiológicas ainda não estão totalmente elucidadas. Nas mitocôndrias vegetais está também presente a proteína desacopladora (UCP) que, por ser capaz de dissipar o gradiente de protões, sob a forma de calor, leva a uma diminuição da produção de ATP, tal como a AOX. De forma a suportar um longo período de tempo em condições ambientais anormais e desfavoráveis,

muitos componentes desta via respiratória não fosforilativa são rapidamente induzidos, o que sugere que estes componentes estão envolvidos na aclimação das plantas e na sua sobrevivência face a essas condições adversas.

Uma vez que, em condições ambientais óptimas, a taxa de oxigenação da Rubisco é entre 20 % a 35 % da taxa de fixação de CO₂, uma enorme quantidade de NADH é produzida na mitocôndria por reacções fotorrespiratórias. E mesmo que a hidroxipiruvato redutase (HPR) no peroxissoma requiera semelhantes concentrações de NADH como aquelas produzidas pelo complexo GDC-SHMT, apenas 30% a 50 % do NADH é exportado da mitocôndria para o peroxissoma, sendo o restante transportado dos cloroplastos. O NADH fotorrespiratório proveniente da mitocôndria pode ser exportado na forma de malato via ciclo malato-oxaloacetato ou malato-aspartato. O restante NADH é oxidado na cadeia respiratória. Neste aspecto as NdiNs e a AOX poderão ter um papel importante já que permitem a oxidação do NADH sem que haja produção de ATP.

Neste trabalho procurou-se testar o papel da AOX na dissipação do potencial redox que ocorre durante a fotorrespiração em condições de stress hídrico. A hipótese proposta é que AOX desempenha aí um papel importante e a sua reduzida actividade se irá reflectir tanto na fotossíntese como na fotorrespiração. Para tal, foram usadas plantas de *Arabidopsis selvagens* (Col-0) e transgénicas exprimindo o gene *AOX1a* em antisense (AS-*AOX1a*). Em *Arabidopsis* as AOX são codificadas por cinco genes, sendo os transcritos de *AOX1a* os mais abundantes nas folhas, em particular, em condições de stress. As plantas foram submetidas a um défice hídrico progressivo, por suspensão de rega e foi monitorizado o estado hídrico do solo (SWC) e o estado hídrico das folhas pela análise do teor hídrico relativo (RWC), potencial hídrico e condutância estomática. Foi igualmente analisada a expressão de um gene de resposta à seca (*RD29A*). Em conjunto, estes dados permitiram o estabelecimento de classes correspondentes a stress suave (S1), moderado (S2) e severo (S3). É de realçar que as plantas em S1 apresentaram um RWC semelhante ao das plantas em condições controlo, embora com uma redução importante no SWC. No entanto o grande aumento da expressão do gene *RD29A* sugere que a resposta à falta de água no solo tenha sido já desencadeada em S1.

Não foram observadas diferenças morfológicas nos dois genótipos estudados, quer em condições controlo quer em stress hídrico. No entanto observaram-se alterações em diversos parâmetros fisiológicos, bioquímicos e moleculares.

Foram também observados valores de Área Foliar Específica e condutância estomática superiores na linha AS em stress moderado, indicando possivelmente uma capacidade diminuída na percepção do stress hídrico e o consequente fecho dos estomas.

As plantas AS-AOX1a apresentaram um menor potencial hídrico para iguais valores de RWC o que parece sugerir uma menor tolerância à seca. Foi curioso verificar que mesmo em plantas bem regadas se observaram valores menores do potencial osmótico nas plantas AS-AOX1a, indicando uma maior concentração de solutos celulares.

Os parâmetros fotossintéticos obtidos a partir de curvas A/C_c mostraram que, tal como esperado, o stress hídrico impôs limitações, quer por danos causados no aparelho fotossintético quer por ajustes metabólicos, que contribuíram para o decréscimo da fotossíntese (A). A taxa máxima de carboxilação da Rubisco (V_{cmax}) registou um decréscimo significativo nas plantas Col-0 que não foi verificado nas plantas AS-AOX1a. Em stress severo, a diferença neste parâmetro entre as plantas Col-0 e as plantas AS-AOX1a foi muito elevada, com as plantas Col-0 a atingirem valores muito baixos, o que indica que estas plantas eram mais limitadas no local de carboxilação da Rubisco para este nível de stress.

Foi ainda detectada uma diminuição na fotorrespiração com o deficit hídrico nas duas linhas de plantas, mas com as plantas AS-AOX1a a atingirem valores menores do que as plantas Col-0 em stress severo. Essa maior diminuição da fotorrespiração nas plantas transgénicas foi reflectida na razão fotorrespiração / fotossíntese, que apesar de não apresentar correlação com o conteúdo de água nas plantas AS-AOX1a, aparentou claramente apresentar valores inferiores quando comparada com as plantas Col-0.

Foi também observado através do decréscimo dos valores de fotossíntese à máxima irradiância e da eficiência quântica da fotossíntese uma forte limitação na cadeia de transporte de electrões na fotossíntese, mas sem diferenças significativas entre as duas linhas de plantas. Foi ainda observado um aumento do ponto de compensação para a luz (maior nas plantas Col-0) com o decréscimo do THR sugerindo igualmente uma actividade (foto)respiratória superior nas plantas selvagens.

Foi possível verificar que F_o e F_m na linha AS sofrera um aumento com o stress enquanto que nenhuma correlação foi observada nas plantas Col-0. O aumento destes parâmetros de fluorescência poderia ter sido causado pelo aumento do conteúdo em clorofilas. No entanto, ocorreu uma diminuição no conteúdo de clorofilas nas plantas AS-

AOX1a. A razão F_v/F_m decresceu ao longo do período de stress possivelmente devido a danos nos centros de reacção do PSII.

Foi ainda possível observar um decréscimo na taxa de transporte de electrões (ETR) à luz saturante, enquanto foi observado um decréscimo nos valores de *quenching* fotoquímico (qP) indicativo de uma maior redução do “pool” de quinonas, mas a forma de variação curvilínea em AS-AOX1a e linear em Col-0 sugere diferenças na dinâmica de sinalização e resposta ao stress. Foi ainda observado um aumento dos valores de *quenching* não-fotoquímico (NPQ). O aumento muito significativo de NPQ, em stress, nas plantas AS-AOX1a, em contraste com o aumento pouco expressivo em Col-0, sugere que nas primeiras estão mais activos mecanismos alternativos de dissipação de energia, o que está de acordo com a suas menores taxas respiratórias. Foi também possível detectar um decréscimo do conteúdo de clorofilas nas plantas AS-AOX1a ao contrário das plantas Col-0 não foi encontrada correlação entre o conteúdo em clorofilas e o stress hídrico. Não foi encontrada correlação entre o conteúdo em carotenoides e o stress hídrico nas duas linhas de plantas devido a grande variabilidade encontrada.

O resultado da análise da expressão génica evidenciou diferenças entre os dois génotipos. Os níveis de expressão inferiores de um gene que codifica uma sub-unidade da glicina descaboxilase (*GDG-P1*) parecem estar de acordo com limitações ao nível da fotorrespiração. Uma tendência semelhante foi observada para a proteína desacopladora (UCP1) cuja função se pensa ser necessária para a eficiência óptima da fotossíntese. Por outro lado níveis de expressão superiores nas plantas AS-AOX1a do gene *SHMT1* poderão surgir como um efeito compensatório, já que nas plantas selvagens se observa um aumento da expressão deste gene em resposta à seca, concomitante com uma diminuição na fotorrespiração.

Os diversos parâmetros estudados mostram que a modificação da expressão do gene *AOX1a*, na linha transgénica, teve repercussões ao nível fisiológico, bioquímico e molecular. Algumas diferenças manifestam-se já em condições controle e muitas outras são observáveis em resposta ao défice hídrico. Em conjunto, os resultados sugerem que as plantas AS-AOX1a ao serem limitadas no aumento da expressão desta isoforma da AOX (que ocorre na selvagem em condições de défice hídrico) apresentam alterações no processo fotorrespiratório.

Abbreviations

$^1\text{O}_2$ - oxygen singlet

a - Area

A - Net photosynthesis at $370 \mu\text{mol m}^{-2} \text{s}^{-1}$

A/C_i - CO_2 assimilation in relation to the intercellular CO_2 concentration

A/C_c - CO_2 assimilation in relation to the chloroplastidial CO_2 concentration

A/I – Photosynthesis / Light curves

ADP - Adenosine diphosphate

A_{max} – maximum photosynthesis rate

AOX - Alternative Oxidase

AOX1a - Alternative Oxidase 1a isoform

AS-AOX1a - Antisense *aox1a Arabidopsis thaliana*

ATP - Adenosine triphosphate

BET - Ethidium bromide

CO_2 - Carbon Dioxide

DNA - Deoxyribonucleic acid

dNTP - Deoxyribonucleotide

DW - Dry weight

EDTA - ethylenediaminetetraacetic acid

ETR - Electron Transport Rate

$F'v/F'm$ - PSII effective photochemical efficiency

Fv/Fm - PSII maximum photochemical efficiency

F_m - Maximum Fluorescence

F_o - Basal Fluorescence

FW - Fresh Weight

GDC - Glycine decarboxylase

GDC-P - Glycine decarboxylase subunit P

gs - Stomatal conductance

H_2O_2 - Oxygen Peroxide

HPR - Hydroxypyruvate Reductase

I - Irradiance

IRGA - Infra-Red Gas Analyzer

J_{max} - Maximum rate of electron transport driving regeneration of RuBP

LCP – Light Compensation Point

LHC – Light Harvesting Complex
NAD(P)H - Reduced nicotinamide adenine dinucleotide
NAD⁺ - Oxydized nicotinamide adenine dinucleotide
NPQ - Non-Photochemical Quenching
O₂ - Oxygen
O²⁻ - Superoxide Anion
OH. - Hydroxyl radical
P/V - Pressure/volume curves
PCD - Programmed Cell-Death
PCR - Polymerase Chain Reaction
PGA - 3-phosphoglycerate
PGly - 2-phosphoglycolate
PSI – Photosystem I
PSII – Photosystem II
qE - Energy-dependent quenching
qP – Photochemical quenching
Rd – Dark respiration
RLT – Lysis buffer
ROS – Reactive Oxygen Species
RPE - Wash buffer
RT-PCR – Reverse Transcriptase- Polymerase Chain Reaction
RubP - Ribulose-1,5-bisphosphate
RW1 - Wash buffer for use with RNeasy kit
RWC – Relative Water Content
Ser - Serine
SHMT - Serine Hydroxymetil Transferase
SLA – Specific Leaf Area
SWC – Soil Water Content
TAE - Tris-acetate and EDTA Buffer
THF - 5,10-methylene tetrahydrofolate
Tm – Melting temperature
TPU – Triose phosphate
TW – Turgid Weight
UCP – Uncoupling Protein
V_{cmax} - Maximum Rubisco carboxylation rate
Φ – Effective quantum yield of PSII electron transport
Ψ_w – Water potential

Ψ_{π} – Osmotic potential

Index

Acknowledgments	2
Abstract	4
Resumo	6
Resumo Alargado	8
Abbreviations	12

1. Introduction	17
1.1. The relation between photosynthesis, respiration and photorespiration	17
1.2. Photosynthesis	17
1.2.1. Drought induced inhibition of photosynthesis	18
1.3. Dissipative processes	18
1.4. Photorespiration as a dissipative mechanism	19
1.4.1. The role of mitochondria in photorespiration	20
1.5. Mitochondrial electron transport chain enzymes	21
1.5.1. Alternative Oxidase	21
1.5.2. AOX genetic expression and regulation	22
1.5.3. AOX functions	22
1.5.4. Uncoupling protein (UCP)	23
1.5.5. UCP genetic expression and regulation	23
1.5.6. Function of UCPs	24
1.6. Mitochondrial photorespiratory enzymes	24
1.6.1. GDC and SHMT structure and regulation	24
1.7. <i>Arabidopsis thaliana</i> as a model for C3 plants	25
1.8. AOX mutants of <i>Arabidopsis thaliana</i>	25
1.9. Objectives	26
2. Materials and Methods	28
2.1. Plant material and growth conditions	28
2.2. Stress conditions and sampling procedures	28
2.3. Water relations	29

2.3.1. Definition of water stress	30
2.4. Photosynthetic parameters	30
2.5. Chlorophyll <u>a</u> fluorescence	31
2.6. Pigment quantification	32
2.7. Gene Expression analysis	32
2.7.1. Bioinformatics analysis	32
2.7.2. RNA extraction and quantification	33
2.7.3. DNA digestion and RNA cleanup	33
2.7.4. Quantification of RNA	34
2.7.5. Reverse Transcription and Polymerase Chain Reaction	34
2.8. Statistical analysis	35
3. Results	36
3.1. Water relations	36
3.2. Photosynthesis and photorespiration	39
3.2.1. A/C _c curves	39
3.2.2. A/I curves	42
3.3. Chlorophyll <u>a</u> fluorescence	43
3.4. Pigment quantification	46
3.5. Gene expression	47
4. Discussion	50
4.1. Water relations	50
4.2. Photosynthesis and photorespiration	52
4.2.1. A/C _c curves	52
4.2.2. A/I curves	53
4.3. Chlorophyll <u>a</u> fluorescence	54
4.4. Pigment quantification	55
4.5. Gene expression	55
5. Conclusion	58
6. References	60
7. Attachments	68

1. Introduction

1.1. The relation between photosynthesis, respiration and photorespiration

Oxidative metabolism interacts with the photosynthetic activity of chloroplasts and this interaction is required for the regulation of the entire cell energy metabolism (Padmasree et al., 2002). In illuminated leaves the metabolism is modulated in a very dynamic way, being dependent on environmental factors and their changes. Under stress conditions the functions of chloroplasts and mitochondria are even more closely coordinated (Noguchi and Yoshida, 2008).

1.2. Photosynthesis

The main function of the light dependent reactions of photosynthesis is to generate ATP and reducing potential in the form of NADPH, required for subsequent carbon reduction. The photochemical apparatus in the thylakoid membrane is composed of two photosystems (PSI and PSII) and an intersystem electron transport chain that encompasses a cytochrome complex (b6/f). The three complexes are linked through plastoquinone and plastocyanin, mobile carriers that diffuse freely within the plane of the membrane. Each photosystem consists of a reaction center and associated antenna with light-harvesting (LHC) complexes. Energy gathered by the antennas' LHCs is passed to the reaction center. There, electron flow is initiated by charge separation (photooxidation). As a result, electrons obtained from the oxidation of water are passed through PSII, the cytochrome complex, and PSI to NADP⁺. Lateral heterogeneity within the thylakoid membranes allow for adjustments to the relative numbers of PSI and PSII and for the output of ATP and NADPH. The carbon reduction occurs in the Calvin cycle which condenses a molecule of atmospheric carbon dioxide (CO₂) with ribulose-1,5-bisphosphate (RuBP) to produce two molecules of 3-phosphoglycerate (PGA) which is then catabolized into ATP and reductants by respiration. ATP and NADPH formed in the light-dependent reactions are required to reduce the product molecules and regenerate the 5-carbon acceptor molecule, RuBP. A key enzyme of the Calvin cycle is ribulose-1,5-bisphosphate carboxylase/oxygenase (Rubisco) which is regulated by light in a very

complex way which involves Mg^{2+} fluxes across the thylakoid, CO_2 activation, chloroplast pH changes and an activating protein (Hopkins, 1999).

1.2.1. Drought induced inhibition of photosynthesis

During drought stomatal closure is induced, regulated by abscisic acid (ABA) and other hormones (Lawlor and Tezara, 2009). Besides the restricted carbon diffusion, metabolic impairment may also pose limitations to photosynthesis. It has been argued that a main target for metabolic limitations is ATP synthesis which in turn could limit RuBP regeneration at mild water deficit (Tezara et al., 1999). Other changes also occur in plant metabolism very early in response to tissue dehydration, maybe as a result of primary and secondary signaling processes like those reported in several molecular studies (for review see Ingram and Bartels, 1996). The idea that non-stomatal mechanisms have a primary role on the limitation of photosynthesis is in conflict with evidence showing that stomatal closure is the major cause for the decline of CO_2 uptake during mild stress. This evidence shows that effects at the chloroplastic level would arise only at tissue relative water content (RWC) below 70% (Kaiser, 1987).

During the onset of drought, stomatal conductance usually drops before photosynthesis, suggesting that the inhibition of photosynthesis under mild stress can be explained by a restriction in CO_2 diffusion (Cornic, 2000). Meyer and Genty (1999) showed that the decrease in the electron transport rate induced by dehydration and ABA treatment, which they thought was mediated by Rubisco deactivation, was almost reverted to the control rate under transient high CO_2 availability. These results suggested that the decline in the intracellular CO_2 after stomatal closure, under prolonged water deficit, would induce an adjustment of the photosynthetic machinery to match the available carbon substrate and the decreased growth. This is also consistent with decreased activity of enzymes of the Calvin cycle, observed when plants growing under field conditions are slowly subjected to a prolonged drought (Maroco et al., 2002).

1.3. Dissipative processes

During drought chloroplasts have systems that dissipate the excess of energy by a non-radiative process which requires conformational changes in PSII. This process can dissipate the energy of about 75% of the photons absorbed by the leaves (Niyogi, 2000).

Under these conditions leaves experience a transient decrease in photochemical efficiency of PSII (Fv/Fm), associated with D1 protein damage at the PSII complex (Powles, 1984). There are two ways of preventing this photooxidation from which superoxide radical (O_2^-) is a byproduct. O_2^- is a reactive oxygen species that can provoke serious damage in plant structures (proteins, lipids and DNA). One way of preventing the accumulation of O_2^- is by scavenging and inactivating it by the action of superoxide dismutase (SOD). SOD can be found in several cellular compartments, and converts O_2^- into hydroxide peroxide (H_2O_2). The H_2O_2 is then reduced to water by sequential reduction with ascorbate, glutathione and NADPH (Hopkins, 1999). Another way of preventing this photooxidation is by trapping and dissipating this excess energy before it reaches the reaction centers. This non-radiative energy dissipation is paralleled by an increase in the concentration of de-epoxidised xanthophyll cycle components at the expense of violaxanthin (Havaux, 1998). One hypothesis is a conformation change of the LHCII, taking place as result of zeaxanthin binding to LHCII has a role in thermal dissipation (Ort, 2001). This conversion of violaxanthin to zeaxanthin and its accumulation requires low pH in the thylakoid lumen (Lawlor and Cornic, 2002). Accumulation of H^+ and concomitant large proton gradient across the thylakoid membrane indicates decreased ATP synthesis. This might occur as a consequence of inadequate regeneration of the substrates ADP or P_i , but it may also occur when ATP synthase is not activated. Such a mechanism explains the strong negative correlation between non-photochemical quenching (NPQ) and ATP under water deficit (Tezara et al., 1999).

1.4. Photorespiration as a dissipative mechanism

Another energy dissipation mechanism present in plants is photorespiration. Due to the competition between CO_2 and O_2 for the catalytic centres of RUBISCO, under atmospheric CO_2 concentrations, part of the RuBP molecular pool may be oxygenated, producing 2-phosphoglycolate (PGly), which can be converted to glycerate in successive reactions (Noguchi and Yoshida, 2008) in the chloroplast, peroxisome and mitochondria. The photorespiration reactions are required for optimal photosynthesis (Padmasree et al., 2002). The mitochondria of higher plants possess many unique components which do not exist in mammalian mitochondria. Among these components is the Glycine decarboxylase (GDC), localized in the mitochondrial matrix and involved in the photorespiratory pathway. GDC complex is strongly induced in the mitochondria of illuminated leaves where GDC and serine hydroxymethyl transferase (SHMT) convert glycine (Gly) and NAD^+ to serine

Even though hydroxypyruvate reductase (HPR) in the peroxisome needs equal amounts of NADH as produced by GDC-SHMT, only 30–50% of NADH is exported from the mitochondria to the peroxisome (Krömer et al., 1995). The remaining NADH required by HPR must be transported from the chloroplasts. Photorespiratory NADH in the mitochondria can be exported in the form of malate from the mitochondria via the Malate–Oxaloacetate shuttle or the Malate–Aspartate shuttle. The rest of the photorespiratory NADH, as shown by Igamberdiev et al. (2001), is oxidized in the respiratory chain. In particular NDin and AOX were proposed to be important for the oxidation of photorespiratory NADH (Igamberdiev et al., 1997).

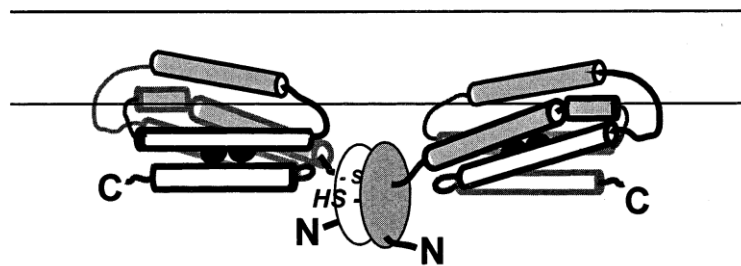


Fig. 12. Structure of alternative oxidase as proposed by Andersson and Norlund (1999) with the monomeric subunits being linked covalently by disulphide bonds. The N-terminal region contains a highly conserved block of amino acids (ovals) which includes the regulatory cysteine. *Adapted from Siedow and Umbach (2000).*

1.5. Mitochondria electron transport chain enzymes

1.5.1. Alternative Oxidase

AOX is an interfacial protein peripherally associated with the matricial side of the internal mitochondrial membrane (Andersson and Nordlung, 1999). The enzyme is present as a dimer in the membrane with the participating subunits of 32KDa linked covalently by disulphide bonds between two conserved cysteine residues (Siedow and Umbach, 2000) (Fig. 12). When the cysteine residues are reduced the disulphide bonds are broken and the monomers can be allosterically activated by α -keto acids, mainly pyruvate through the formation of a thiohemiacetal by reaction between the cysteine sulfhydryl and the α -keto-acid (Siedow and Umbach, 2000). When alternative oxidase is activated by pyruvate it can compete with the cytochrome chain for electron flux and does so most effectively under adenylate-limited conditions. Accumulation of pyruvate during glycolysis will not

only ensure that activation of the alternative oxidase occurs, but also that it contributes to respiration. Glyoxylate is also an activator of the alternative oxidase and, therefore, the oxidase is likely to be activated during photorespiration (Hoefnagel et al., 1995).

1.5.2. AOX genetic expression and regulation

In higher plants AOX protein is encoded by a small multigenic family with two groups of genes, the *Aox1* and *Aox2* genes. The expression of each of these genes can vary according to the developmental stage of the plant (Vanlerberghe and McIntosh, 1997). Several studies have shown that *Aox1* genes are specially expressed as a response to stress conditions and exist both in monocots and dicots. Some reports also indicates that *Aox2* genes, which have been detected only in dicots, also function in stress-response (Clifton et al., 2005; Costa et al., 2007; Matos et al., 2009).

1.5.3. AOX function

Several physiological roles have been proposed for AOX, however, there isn't a consolidated scientific statement about its real function. Initially, having been discovered in Aracea in a thermogenic tissue, the AOX function was thought to be to generate heat thereby dissipating volatile pheromones produced to attract pollinator insects. However, the discovery of AOX in non-thermogenic plants suggested that this protein has additional functions.

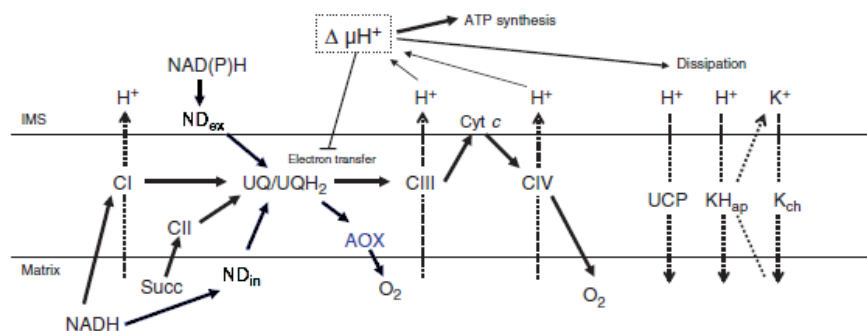


Fig. 13. Energy dissipating systems in a plant mitochondrial membrane. The pathways of electrons from the substrates to oxygen via the different complexes of the mitochondrial respiratory chain are represented with bold arrows and the coupled export of protons with dotted arrows. NDin, internal NADH dehydrogenase; NDex External NADH dehydrogenase; AOX, alternative oxidase; UCP, uncoupling protein; KHap, K^+/H^+ antiporter; Kch, potassium channel. Adapted from Atkin and Macherel (2009).

It was suggested that AOX might act as a mechanism of energy overflow allowing a deviation of the electron flux from the cytochrome pathway upon saturation or when the

ATP/ADP ratio was high above physiological values (Lambers, 1982) (Fig. I3). Later, in 1995, Hoenfnagel and collaborators suggested that AOX in the presence of pyruvate can compete for the electrons with cytochrome c oxidase even when this pathway isn't saturated. According to the AOX regulation mechanisms previously discussed, changes that result in the accumulation of reduced quinones, reduced mitochondrial pyrimidine nucleotides or other organic acids, have the ability to enhance AOX activity. And so electron flux can be regulated so that the transport occurs through the cytochrome or the alternative pathways. This mechanism fits the requirements of cells that need to produce carbon skeletons without raising the intracellular levels of ATP, as the use of alternative pathways allows the function of the citric acid cycle with less production of ATP (Simons et al., 1999).

On the other hand, AOX prevents the over-reduction of the components of the respiratory chain that would otherwise result in the accumulation of ROS (Maxwell et al., 1999; Umbach et al., 2005). ROS can promote cell death through oxidative stress in mitochondria. These molecules also act as signaling compounds of programmed cell death (PCD) and necrosis. The global mechanism of plant PCD is yet unknown although it shows some similarities with animal apoptosis (Aranha et al., 2006). Besides preventing ROS accumulation, a delay of necrosis has also been associated with AOX (Simons et al., 1999).

1.5.4. Uncoupling Protein (UCP)

Similar in function to AOX in decreasing ATP formation, is UCP, a transmembrane protein which dissipates the proton gradient (Krauss et al., 2005). UCP was firstly discovered in animals, in brown adipose tissue where it contributes to heat generation. Recently these proteins were also discovered in plants. In plants and animals, UCPs are coded in the nuclear genome by multigenic families. *Arabidopsis thaliana* UCPs family is so far the only one characterized, where 6 putative genes were identified: AtUCP1, AtUCP2, AtUCP3, AtUCP4, AtUCP5, AtUCP6 (Maia et al., 1998; Borecký, 2006).

1.5.5. UCP genetic expression and regulation

It was firstly suggested that UCP genes could also be stress responsive, mainly to low temperature.(Maia et al. 1998; Seki et al. 2002). More recently Borecký et al. (2006) observed, in *Arabidopsis*, that UCP1, UCP4 and UCP5 genes are constitutively expressed, being the transcripts of the last two more abundant.

1.5.6. *Function of the UCPs*

UCP activation is dependent on free on fatty acids and purine nucleotides are inhibitors of these proteins. Recent evidence also suggests that the activity of plant UCPs is stimulated by ROS (Smith et al., 2004). Although UCPs activities might lead to heat generation, it is not believed that their presence in plants serves that purpose (Sweetlove et al., 2006). The proton electrochemical gradient energy dissipating pathway involving UCPs leads to the same effect as the alternative oxidase pathway, which is a decrease in the efficiency of oxidative phosphorylation and an increase in heat production (Hourton-Cabassa et al., 2004; Nunes-Nesi et al., 2008). Both systems were proposed to play a role in protecting plant cells against oxidative stress. Transgenic plants with higher levels of AtUCP1 are more tolerant to oxidative stress (Brandalise et al., 2003).

1.6. Mitochondrial photorespiratory enzymes

1.6.1. *GDC and SHMT structure and regulation*

The complex glycine decarboxylase-serine hydroxymethyltransferase (GDC-SHMT) is located within the mitochondrial matrix. GDC is a mitochondrial multienzyme complex which consists of four different component enzymes: P-, H-, T- and L- proteins involved in photorespiration and one-carbon metabolism, in all photosynthesizing organs and in all biosynthetically active tissues (Douce et al., 2001). In Arabidopsis there are two isoforms of P- proteins of GDC. The role of the proteins was studied by Engel et al. (2007), who concluded that only the knockout of both isoforms of P- proteins arrested the development of the cotyledon stage even under non-photorespiratory conditions. This suggested that GDC activity is required for other processes apart from photorespiration.

Regarding SHMT, seven proteins have been identified, SHMT1-7 in Arabidopsis (Bauwe and Kolukisaoglu, 2003). In the C2 cycle the complex is involved in the reversible interconversion of serine and glycine and both enzymes are closely associated with each other. During the C2 cycle, one molecule of glycine is first decarboxylated and subsequently deaminated in the glycine decarboxylase complex yielding CO₂, NH⁴⁺, and the C1 donor, 5,10-methylene tetrahydrofolate (THF), which is used by SHMT to transfer the activated C1 unit to another molecule of glycine (Voll et al., 2006).

Like GDC, SHMT is involved in the reversible interconversion of serine and glycine (Voll et al., 2006), and plays a role in controlling cell damage caused by biotic stress most likely because photorespiration is part of the dissipation mechanism that mitigates oxidative damage (Nunes-Nesi et al., 2008). *AtSHM1* appears to encode the major isoform in Arabidopsis leaves and its transcript level is regulated by light and the circadian clock. *SHMT2* is predominantly expressed in roots and in the shoot apical meristem (Voll et al., 2006). *SHMT1* mutants cause aberrant regulation of cell death resulting in chlorotic and necrotic lesion formation under a variety of environmental conditions. Salicylic acid-inducible genes and genes involved in H₂O₂ detoxification were expressed constitutively in these plants in direct correlation with the severity of the lesions (Moreno et al., 2005).

1.7. *Arabidopsis thaliana* as a role model for C3 plants

Arabidopsis is a small flowering plant, native from Europe, Asia and north Africa and is widely used as a model organism in plant biology. Arabidopsis is a dicotyledonous species, a member of the Brassicaceae family. Although closely related to such economically important crop plants such as turnip, cabbage, broccoli, and canola, Arabidopsis is not an economically important plant (Meinke et al., 1998).

Arabidopsis genome is organized into five chromosomes (Meinke et al., 1998) fully sequenced in 2000 (Tabata et al., 2000). Besides this overwhelming step in plant molecular biology, Arabidopsis has other traits that are a benefit for a plant model. It has a rapid life cycle and produces numerous self progeny. It has very limited space requirements, and is easily grown in a greenhouse or indoor growth chamber. The genome can also be manipulated through genetic engineering more easily and rapidly than any other plant genome (Flavell, 2009). Currently there are a wide number of transformed plants available.

1.8. *AOX* mutants of *Arabidopsis thaliana*

Fiorani et al. (2005) using *AOX1a* anti-sense line of Arabidopsis (Umbach et al., 2005) observed, at low temperature, impairments in plant development reflected in reduced rosette sizes and specific leaf area which did not seem to result from alterations the redox state of the tissue, as no differences were found in the content of lipid peroxidation

products and transcripts of genes encoding antioxidant enzymes. These differences were, however, correlated with the amount of shoot anthocyanins at low temperature and with the transcription of flavonoids pathway genes. These results indicate that AOX is required for acclimation to low temperature in *Arabidopsis* not only through local effects in mitochondria but rather through extramitochondrial effects on metabolism.

The effect of the lack of AOX1a on the response to low temperature in *Arabidopsis* was also studied by Watanabe et al. (2008), using a T-DNA insertion line. Under low temperatures, AOX1a RNA was strongly induced in wild type plants. The transformed plants, unable to up-regulate AOX1a, but displaying increased cyanide-resistant respiration showed increased UCP1 and NDext expression. The authors also observed that the lack of AOX was linked to a difference in the carbon/nitrogen balance and an up-regulation of the transcription of antioxidant defense systems at low temperatures. In contrast to the growth reduction observed in the antisense plants (Fiorani et al. 2005), no cold-related morphologic phenotype was observed in the T-DNA line (Watanabe et al. 2008). Also using a T-DNA insertion line in the AOX1a gene of *Arabidopsis* Giraud et al. (2008) observed a phenotypic difference. Under combined stresses, consisting of moderate light plus drought, the T-DNA mutants accumulated more anthocyanins, O_2^- and had increased NPQ values compared to the wild-type plants. The combined stresses resulted also in alterations in abundance of a variety of transcripts such as mRNAs encoding enzymes related to anthocyanin synthesis, cell wall synthesis, transcriptions factors, chloroplastic and mitochondrial components, among others, indicating that the effects of the mutation were not only confined to mitochondria. More recently T-DNA *aox1a* plants did not show any phenotype under normal growth conditions, but after inhibition of the cytochrome pathway by antimycin A (which induces AOX1a expression in the wild-type), inhibition of photosynthesis, increased ROS formation and membrane leakage were observed (Strodtkotter et al., 2009)

Taken together these results indicates that plants with reduced or absent expression of AOX1a have a greatly altered stress response even when the mitochondria is nor the primary target of the stress and suggests that AOX1a plays a important role in cell metabolism perhaps by a role related to the redox balance in the cell.

1.9. Objectives

This work aims to test if AOX has a role in the mitochondrial redox potential dissipation that occurs during photorespiration under water stress conditions. The hypothesis is that AOX plays an important role and its lower activity will reflect itself in photosynthesis and photorespiration.

Wild type (Col-0) *Arabidopsis* and *AOX1a* transgenic *Arabidopsis* (AS-*AOX1a*) (Umbach et al., 2005) will be submitted to progressive water deficit in order to achieve mild, moderate and severe water stress, previously known to induce the up-regulation of *AOX1a* gene (A.R.Matos, unpublished results). The relationship between photorespiration and photosynthesis in control and water stress conditions will be studied in Col-0 and AS-*AOX1a* plants.

2. Materials and Methods

2.1. Plant material and growth conditions

Seeds of *Arabidopsis thaliana* (L.) Heynh. ecotype Columbia (Col-0) were used as the wild type along with a transgenic line (AS-AOX1a) expressing the *AOX1a* gene in antisense, under the control of the CaMV 35S promoter. The transgenic line was generated by Umbach et al. (2005) and the seeds (CS6599) were made available from TAIR, <http://www.arabidopsis.org/>. The plants were grown in a walk-in chamber with the photoperiod set to 10/14h (day/night) with a light intensity of 170-180 $\mu\text{mol m}^{-2} \text{s}^{-1}$ and the temperature to 23/18°C (day/night). The relative humidity (RH) was maintained at 40-70% with a humidification device (S&P Humi-3E, HM-204). The light intensity was periodically checked with a radiometer (Quantum Meter, Apogee Instruments, Inc) and the temperature and humidity permanently recorded with a HOBO (Onset HOBO RH, temperature Data Logger, Onset).

Plants were grown in 200 cm³ pots with a mixture of commercial soil (Combo Sana) and vermiculite (1:1), previously sterilized for 4 hours in an oven at 190°C. The seeds were surface sterilized with a solution of ethanol 95% for 3 minutes, followed by a wash of 20% (v/v) sodium hypochlorite and 0,1% (w/v) tween 20 (1mL for \pm 100 seeds) for 3 minutes. Five sequential washes of 1 min were made with MilliQ water. To synchronize germination the seeds were stratified at 4°C for 4 days after imbibition.

Three seeds were planted per pot and placed in a tray, covered with a transparent plastic film in order to keep a water saturated atmosphere during germination. To avoid the influence of micro-habitats effects the trays were rotated every day. The plants were germinated at a light intensity of 60-70 $\mu\text{mol m}^{-2} \text{s}^{-1}$ for two weeks after which holes were made in the plastic film and 2 of the 3 plants in each pot were removed. The most developed plant was left. At this time the plants were changed to a light intensity of 170-180 $\mu\text{mol m}^{-2} \text{s}^{-1}$ and watered by sub-irrigation with deionized water every two or three days.

2.2. Stress conditions and sampling procedures

Water deficit was imposed by withholding watering to 30-35 day-old plants. The samples

were collected taking into account the days of water withholding and the visual aspect of the plants. Control plants were kept well watered, by sub-irrigation, every two or three days. Control plants were tested in the same days as stressed plants. For all parameters examined, control samples were collected over time to monitor the effect of plant age. However, gene expression was analyzed only on an initial and on a final control, since only a limited number of samples can be analyzed simultaneously by this method. Plants were always photographed before sampling.

Fully expanded leaves were used in the experiments. These were either immediately assayed, detached or not from the plant, or collected, immediately frozen in liquid nitrogen and stored at -70°C, depending on the type of experiment.

2.3. Water relations

Soil water status was evaluated by soil water content (SWC), which is the percentage of water in the soil (Coombs et al. 1987). The equation used was:

$$\text{SWC (\%)} = 100 \times [(\text{FW} - \text{DW}) / (\text{FW})]$$

where FW is the fresh weight of the soil and DW is its dry weight, measured after drying at 120°C for 24 hours in an oven (Memmert, Schwabach, Germany).

The leaf relative water content (RWC) was measured according to Catsky (1960). The equation used was:

$$\text{RWC (\%)} = 100 \times [(\text{FW} - \text{DW}) / (\text{TW} - \text{DW})]$$

where FW is the leaf fresh weight, TW is the turgid weight of a leaf sample and DW is its dry weight. TW was obtained by floating the leaves in a closed petri dish with deionized water (with the adaxial phase in contact with the water) overnight. DW was measured after drying in an oven (Heraeus D-6450 Hanau) at 70 °C for 48 hours.

Specific Leaf Area (SLA) was calculated using the leaf area (a) (measured with a leaf area meter (CI-202 Portable Area Meter, ENVCO)) and its dry weight as shown in the following equation:

$$\text{SLA (Specific Leaf Area)} = a/DW$$

Water Potential (Ψ_w) was measured on a leaf disk with a 0,5 cm diameter. It was determined with a C-52 chamber connected to a HR33 Dew Point microvoltmeter (Wescor Inc., Logan, UT, USA), allowing 30 min of equilibration after enclosing the disk in the chamber.

For the osmotic potential (Ψ_π) another leaf (of similar size) was detached and frozen in liquid nitrogen and stored at -70 °C (Harris A-45605C) to destroy cell membranes. Discs were cut from the leaf and measured as indicated for Ψ_w .

2.3.1. Definition of water stress classes

For some data analysis purposes, the results were grouped in 3 water stress levels: S1, mild water stress, corresponding to RWC between 75 and 60 %; S2, moderate water stress, corresponding to RWC between 60 and 40 %; and S3, severe water stress, corresponding to RWC lower than 40%.

2.4. Photosynthetic parameters

Photosynthetic gas exchange measurements were performed in undetached fully expanded leaves using a portable infra-red gas analyzer (IRGA, LCpro+ ADC BioScientific Ltd., Herfordshire, UK) with controlled leaf chamber atmosphere. The net CO₂ assimilation rate (A) and stomatal conductance (gs) of Arabidopsis leaves were determined under a controlled atmosphere with approximately 370 $\mu\text{mol mol}^{-1}$ CO₂, relative humidity (RH) of 60-70 %, temperature of 25±2 °C and a saturating external light source of 600 $\mu\text{mol m}^{-2}\text{s}^{-1}$ set by an external controllable LED light unit (ADC BioScientific Ltd, Herfordshire, UK).

Photosynthetic carbon dioxide response curves were performed under similar atmosphere conditions (RH 60-70%, 25°C, 600 $\mu\text{mol m}^{-2}\text{s}^{-1}$ of irradiance) but different CO₂ partial pressure, according to Long and Bernacchi (2003). In leaves pre-adapted to 370 $\mu\text{mol mol}^{-1}$ of CO₂ for 10 minutes, measurements were taken during 5 minutes for each CO₂ concentration: firstly by a stepwise decrease of the CO₂ concentration from 370 to 100 $\mu\text{mol mol}^{-1}$ CO₂ and, secondly, restoring the initial CO₂ value of 370 $\mu\text{mol mol}^{-1}$ CO₂ followed by a stepwise CO₂ increase up to 1500 $\mu\text{mol mol}^{-1}$ CO₂. The leaf internal CO₂ partial pressure (C_i) and A were recorded and the last one corrected for the leaf area.

After the measurements were taken, the leaf was used for RWC determination. Fitting an A/C_i curve the mesophyll conductance (g_m) was estimated and the CO_2 partial pressure inside the chloroplast (C_c) determined according to Farquhar et al. (1980) and Sharkey et al. (2007). The maximum Rubisco carboxylation rate (V_{cmax}), the maximum rate of electron transport driving regeneration of RuBP (J_{max}) and the rate of use of the triose-phosphates (TPU) were calculated from the A/C_c curves according to Sharkey et al. (2007) and using the estimator utility found at <http://www.blackwellpublishing.com/plantssci/pcecalculation/>.

Photosynthesis light curves were performed at ambient CO_2 concentrations (approximately $370 \mu\text{mol mol}^{-1} CO_2$), RH of 60-70 %, 25 ± 2 °C and different irradiance (I). In leaves dark-adapted for 5 minutes, measurements were recorded also during 5 minutes at each irradiance, light intensities rising stepwise from 100 to $1600 \mu\text{mol m}^{-2} \text{s}^{-1}$. Once again, A was corrected for the leaf area. The photosynthetic apparent quantum yield (Φ) was estimated as the initial slope of the A/I curve, the rate of dark respiration (R_d) was the intercept with the y-axis, the apparent light compensation point (LCP, the light value at which the rate of CO_2 fixation by photosynthesis is similar to the rate of CO_2 release by respiration and photorespiration) was the intercept with the x-axis and maximum photosynthesis rate (A_{max}) was given as the asymptotic A value as irradiance tends to infinity, according to Lambers et al. (1998). Using some of these previously estimated parameters, A/I curves' further statistical analysis allowed the determination of A_{max} , ϕ and R_d , using SPSS 17.0 statistical software (SPSS Inc., Chicago, IL, USA).

Photorespiration rate was determined according to Sharkey (1988), in leaves under $370 \mu\text{mol mol}^{-1} CO_2$, relative humidity of 60–70% and 25 ± 2 °C and a saturating external light source of $600 \mu\text{mol m}^{-2} \text{s}^{-1}$, using the respective g_m and R_d calculated from A/C_i curve performed and analyzed as described.

2.5. Chlorophyll a fluorescence

Chlorophyll a fluorescence was measured in a PAM 210 (Heinz Walz GmbH, Effeltrich, Germany). The PAM 210 fluorometer was connected to a computer and operated under the software DA-Teach in basic mode (Marques da Silva et al., 2007). Minimal fluorescence (F_o), maximal fluorescence (F_m) and the maximum photochemical efficiency of PSII (F_v/F_m) were recorded after 10 minutes of dark adaptation. Effective quantum yield of PSII (Y), electron transport rate (ETR), chlorophyll fluorescence photochemical quenching (qP) and non-photochemical quenching (NPQ) were measured after 10 minutes

at $200 \mu\text{mol m}^{-2} \text{s}^{-1}$ and again after another 10 minutes at $600 \mu\text{mol m}^{-2} \text{s}^{-1}$, as were also the respective F'_o and F'_m . F'_v/F'_m was calculated according to Baker and Rosenqvist (2004).

2.6. Pigment quantification

After measuring chlorophyll fluorescence, each leaf was weighed and immersed in 10 mL of methanol for pigment extraction and kept in the dark, at room temperature, for at least 48 hours (or until the leaf turns white). Spectrophotometric measurements (Unicam 500 β UV/Vis Spectrometer, Unicam, Cambridge, UK) were taken at 470nm, 652,4nm and 665,2nm to determine chlorophyll *a*, chlorophyll *b* and carotenoids concentrations according to Lichtenthaler (1987).

Anthocyanin quantification was adapted from Giraud et al. (2008) using the same extracts. After photosynthetic pigment determination 2N HCl was added to obtain a dilution of 1% (v/v). Total anthocyanins were determined as the difference between absorbance at 530nm (A_{530}) and 657nm (A_{657}):

Anthocyanins relative content $\text{g}^{-1} \text{DW} = (A_{530} - (0,25 * A_{657}) * \text{extraction volume}) / \text{DW}$

2.7. Gene Expression analysis

2.7.1. Bioinformatics analysis

Primer choice is crucial for a good RT-PCR amplification. For the genes to be tested: *UCP1* (AT3g54110), *UCP2* (AT5g58970), *UCP4* (At1g14140), *SHM-1* (AT4g37930) and *RD29A* (AT5g52310); the sequences were obtained through TAIR (<http://www.arabidopsis.org/>). To ensure that the primers (Table 1.) amplified only the desired gene, the cDNA sequences from the genes belonging to the same family or closely related families, in *Arabidopsis thaliana*, were searched through a blast against the Arabidopsis database (<http://blast.ncbi.nlm.nih.gov/Blast.cgi>). Multiple sequences alignments were performed by Clustalw (<http://www.ebi.ac.uk/Tools/clustalw2/index.html>) and primers were selected in low homology regions and encompassing introns, whenever possible, as an additional precaution to distinguish from genomic DNA PCR products. Primers for *GDC-P1* (AT4g33010.1) were previously described by Engel et al. (2007).

Table 1. Genes studied in the present work. Number of cycles, primers used for cDNA amplification, the respective T_m and expected size of the PCR product. *UCP*, uncoupling proteins 1, 2 and 4; *SHMT-1*, serine hydroxymethyl transferase protein 1; *GDC-P1*, protein P1 of glycine decarboxylase; *RD29A*, responsive to desiccation 29A; FW Primers, forward primers; RV Primers, reverse primers.

Gene	T _m (°C)	Cycles	FW Primers	RV Primer	Size of PCR product (bp)
<i>UCP1</i>	68	28	GTAAATTCGACCTTTCCTTGCCCA	TTCTGGCCTCTCTCAATCACCGAA	985
<i>UCP2</i>	61	45	CAATGGCGGATTTCAAACCAAGGAT	ATCGTACAAGACTTCTCTTAGAAAC	917
<i>UCP4</i>	61	45	GGTAATCAAATCCGGTAAAATGGAG	CACAAAGCTCTTATTCCCTCAAACCT	835
<i>SHMT-1</i>	61	45	TCAGAAAGGTCGTGAACAAGC	AGTATATTTCTTTTGATGTATAGA	971
<i>GDC-P1</i>	68	20	TCATGCTCAAGCGTTGCTTG	AGTGGTTGAGTCCACAACAC	256
<i>Rd29A</i>	60	22	AAGAAACTGGAGGAGTACC G	TTGGGCTCTCCAGCTCA	681

2.7.2. RNA extraction and quantification

For RNA extraction, previously weighed frozen leaves were used according to Qiagen RNeasy Kit protocol. The tissue was thoroughly ground in liquid nitrogen with a mortar and pestle. The tissue powder was decanted into an RNase free microcentrifuge tube. 450 µL of RLT buffer were added to the microtube and then vortexed for 1-3 seconds. The lysate was transferred to a QIAshredder spin column (provided with the kit) placed in a 2 mL collection tube and then centrifuged (Sigma, 2-16 K) for 2 min at full speed. The supernatant of the flow-through was carefully transferred to a new microtube. After this, 50% of volume of ethanol (96-100%) was added. The samples were then transferred to an RNeasy spin column (provided with the kit), placed in a 2 mL microtube and then centrifuged for 15 seconds at ≥8000 g. The flow-through was discarded. 700 µL of RW1 buffer were added to the RNeasy spin column and centrifuged for 15 seconds at ≥8000 g. The flow-through was discarded. 500 µL of RPE Buffer were then added to the RNeasy spin column and centrifuged as before. Again the flow-through was discarded. Another 500 µL of Buffer RPE were added to the RNeasy spin column and centrifuged for 2 minutes at ≥8000 g. The RNeasy spin column was placed in a new 2 mL microtube and centrifuged at full speed for 1 minute. The flow-through was discarded and the RNeasy spin column placed in a 1,5 mL microtube and 50 µL of RNase-free water were added and then centrifuged at ≥8000 g for 1 minute.

2.7.3. DNA digestion and RNA cleanup

DNA digestion was made “in column” after adding the 700 μL of RW1 buffer and before adding the 500 μL of RPE Buffer during the extraction.

350 μL of RW1 buffer were added to the RNeasy spin column and centrifuged for 15 seconds at $\geq 8000\text{ g}$. The flow-through was discarded. Afterwards, 218 U of DNase1 (Qiagen) were added and left to incubate at 20-30 $^{\circ}\text{C}$ for 15 minutes. 350 μL of RW1 buffer were added to the column and again, centrifuged for 15 seconds at $\geq 8000\text{ g}$ and the flow-through was discarded.

2.7.4. *Quantification of RNA*

RNA concentration was determined by spectrophotometry (Unicam 500 β UV/Vis Spectrometer, Unicam, Cambridge, UK) at 260 nm. The concentration was determined assuming that 1 absorbance unit corresponds to 40 ng/ μL of RNA.

Working solutions were made with a concentration of 50 ng/ μL and 10 ng/ μL of RNA. The dilutions of the different RNA samples were verified by electrophoresis (Mini-Sub Cell GT, BioRad, powered by Power Pac Basic, BioRad) in a 2% agarose gel with 0,0001% of ethidium bromide in TAE buffer (40 mM Tris-acetate; 1mM EDTA, pH 8,3) and photographs taken with Gel-doc XR Imaging System (BioRad).

2.7.5. *Reverse Transcription and Polymerase Chain Reaction*

Reverse transcription (RT) allows obtaining the complementary DNA from RNA in a reaction catalyzed by a reverse transcriptase. The product is then amplified by a Taq polymerase in a polymerase chain reaction (PCR) (MJ Mine, Personal thermal cycler, BioRad). The PCR conditions were: 30 minutes at 50 $^{\circ}\text{C}$ (reverse transcriptase step), 15 minutes at 95 $^{\circ}\text{C}$ (inactivation of the reverse transcriptase and Taq activation step), a 3 step cycle (30 sec at 95 $^{\circ}\text{C}$ for denaturation, 30 sec at appropriate T_m for annealing and 1 minute at 72 $^{\circ}\text{C}$ for extension) multiplied by the number of cycles determined for each gene.

In order to determine the ideal number of cycles for each gene, allowing the visualization of PCR products in ethidium bromide (BET) stained gels and preventing saturation, a RT-PCR mix was prepared with 5 μL buffer 5x, 1 μL dNTP (10 mM each), 1,5 μL FW primer (10 pmol/ μL), 1,5 μL RV primer (10 pmol/ μL), 1 μL enzyme mix and 10 μL of RNA (10ng/ μL or 50ng/ μL) and RNase-free water up to a final volume of 25 μL accordingly to the OneStep RT-PCR kit (Qiagen). Five μL samples were taken at cycles 25, 30, 35, 40 and after a final extension (10 minutes at 72 $^{\circ}\text{C}$). The PCR products were visualized by

electrophoresis as above described.

To analyze gene expression in the different RNA samples prepared from control and stressed leaves of WT and transgenic line a mastermix was prepared as detailed above and the total reaction volume for each sample was of 12.5 μL , containing 5 μL of the RNA solution.

2.8. Statistical analysis

The relations between different parameters were tested by regression analysis in the program GraphPad Prism 5. The F-test allowed the choice of regression model (linear or quadratic) that fitted best to the data group being evaluated. The probability of the linear regression being significant was estimate by r^2 critical values. An overall quadratic regression was assumed to be significant whenever a linear regression on the same data set was significant. Otherwise, an overall significance test of quadratic regressions was applied, treating them as a 2 independent variable multiple linear regressions and performing a Variance Ratio test, according to Daniel (1987). Differences on the slopes of linear regressions and on the entire set of points of quadratic regressions were tested with the program GraphPad Prism 5 by analysis of covariance and the extra sum-of-squares F test. Whenever necessary, t-tests were applied to test for significant differences on the mean value of Col-0 and AS-AOX1a physiological parameters at selected levels of stress. Significant differences were accepted for $p < 0,05$, except when specifically stated otherwise.

3. Results

Several experiments were done with the two lines of *Arabidopsis* (Col-0 and AS-AOX1a) in irrigated (control - C) and water deficit (stress - S) conditions in order to study the relation between photorespiration and photosynthesis under water stress and the possible role of AOX is in this relation.

3.1. Water relations

In order to choose the parameter that better reflects the water stress status of the plants, net photosynthesis measured at $375 \mu\text{mol mol}^{-1} \text{CO}_2$ (A) was analyzed in function of RWC, stomatal conductance (g_s) and water potential (Ψ_w) (Fig. 1). This experiment was conducted with the Col-0 plants in order to avoid possible metabolic constrictions from the AS-AOX1a plants. All three correlations are statistically significant but unlike the relation A Vs RWC and A Vs Ψ_w , the relation A Vs g_s is not linear (Fig. 1).

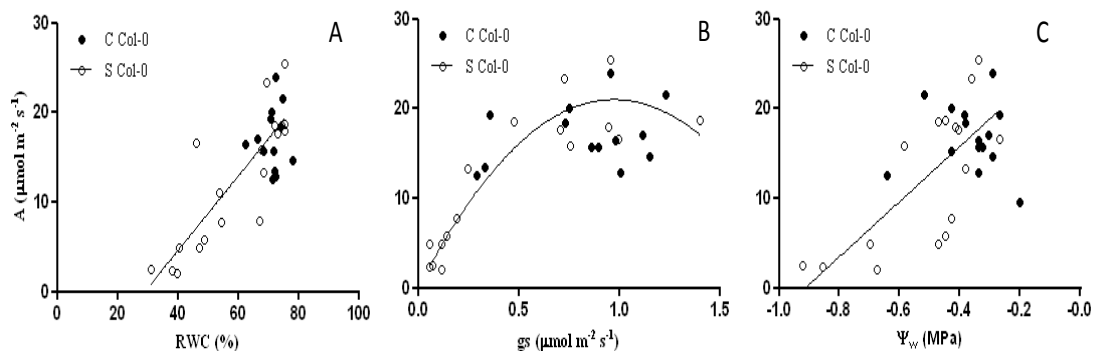


Fig. 1. Relation between A and RWC (A); g_s (B) and Ψ_w (C) in Col-0 *Arabidopsis* under control (C) and stress (S) conditions. A: $r^2=0,7202$ $p<0,05$; B: $R^2=0,869$ $p<0,05$; C: $r^2=0,526$ $p<0,05$.

Photographs were taken to visualize the phenotype of the Col-0 (Fig. 2, A - E) and the AS-AOX1a (Fig. 2, F - J) plants. Three levels of drought stress were selected: mild stress (S1, RWC = 60-75 %) (Fig. 2, B and G), moderate stress (S2, RWC = 40-60 %) (Fig. 2, C and H) and severe stress (S3, RWC < 40 %) (Fig. 2, D and I) as well as two controls one at the beginning (Fig. 2, A and F) and the other at the end of the experiment (Fig. 2, E and J).

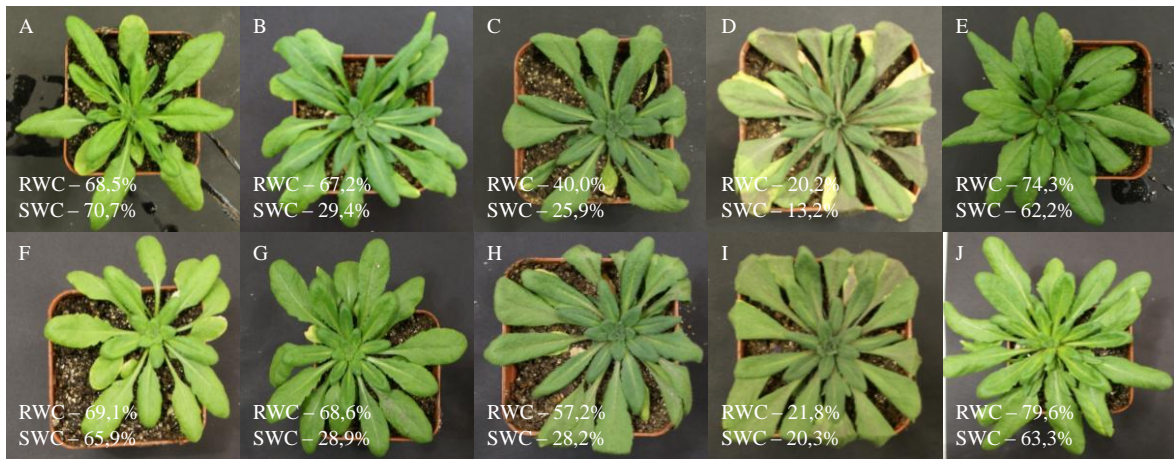


Fig. 2. Visual aspect of *Arabidopsis* plants during a stress cycle. A, B, C, D and E are Col-0 plants; F, G, H, I and J are AS-AOX1a plants. A and F are control plants at the beginning of the stress cycle. E and J are control plants at the end of the stress cycle. B and G are plants subjected to mild stress (S1). C and H are plants subjected to moderate stress (S2). D and I are plants subjected to severe stress (S3).

It is worthwhile to note that although S1 plants (Fig. 2, B and G) shows the same RWC as the control plants at the beginning of the stress cycle (Fig. 2, A and F), the SWC of their pots was much lower (results not shown). This indicates that a major amount of water may be lost from the soil before any changes in leaf RWC is found.

A significant linear decrease of the Specific Leaf Area (SLA) with stress was found for both lines of *Arabidopsis* ($p < 0,05$), without any significant differences in the relation SLA / RWC between Col-0 and AS-AOX1a plants ($p > 0,05$) (Fig. 3). However, the values of SLA seem to drop sharply at mild water stress for the Col-0 plants, whereas in moderate and severe stress they remain relatively stable as the RWC continues to decrease (Fig. 3). In fact, at mild water stress the mean SLA of Col-0 ($476,7 \pm 55,7 \text{ cm}^2 \text{ g}^{-1} \text{ DW}$) is significantly lower than the mean SLA of AS-AOX1a ($552,2 \pm 74,23 \text{ cm}^2 \text{ g}^{-1} \text{ DW}$) ($p < 0,05$), while for the control and the other stress levels no differences between the mean SLA of Col-0 and AS-AOX1a were found (Fig. 3).

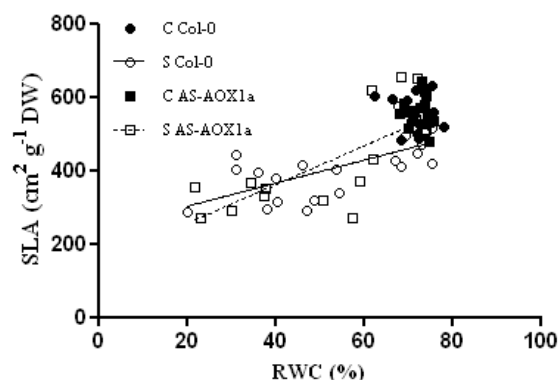


Fig. 3. Relation between SLA and RWC in Col-0 and AS-AOX1a under control and stress conditions. C – control; S – stress. Col-0 - $r^2=0,46$ $p < 0,05$; AS-AOX1a $-r^2=0,585$; $p < 0,005$. No statistical differences on the slope SLA / RWC were found between Col-0 and AS-AOX1a ($p > 0,05$).

A significant curvilinear decrease of Ψ_w with decreasing RWC ($p < 0,05$) was found for both lines of Arabidopsis (Fig. 4A). Furthermore, a statistically significant difference was found between the fits for Col-0 and AS-AOX1a plants ($p < 0,05$) indicating that the Ψ_w of AS-AOX1a is lower than the Ψ_w of Col-0. In fact, the mean Ψ_w of control AS-AOX1a plants ($-0,45 \pm 0,06$ MPa) is significantly lower than the mean Ψ_w of control Col-0 plants ($-0,37 \pm 0,11$ MPa) ($p < 0,05$). Also under severe water deficit the mean Ψ_w of AS-AOX1a plants ($-1,08 \pm 0,19$ MPa) is significantly lower than the mean Ψ_w of Col-0 plants ($-0,82 \pm 0,10$ MPa) ($p < 0,05$).

A significant curvilinear decrease of Ψ_π with decreasing RWC ($p < 0,05$) was found for both lines of Arabidopsis (Fig. 4B), without significant differences between their fits ($p > 0,05$) (Fig. 4B), in spite of control AS-AOX1a plants having lower mean Ψ_π values ($-0,47 \pm 0,06$ MPa) than the control Col-0 plants ($-0,37 \pm 0,11$ MPa) ($p < 0,05$).

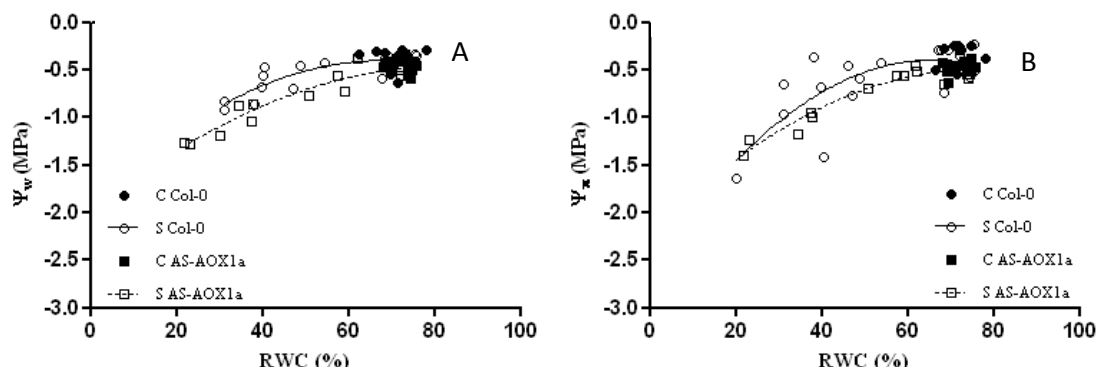


Fig. 4. Relation between Ψ_w (A), Ψ_π (B) and RWC in Col-0 and AS-AOX1a under control and stress conditions. C – control; S – stress. A: Col-0 $R^2=0,737$ $p < 0,05$; AS-AOX1a $R^2=0,923$ $p < 0,05$; B: Col-0 $R^2=0,565$ $p < 0,05$; AS-AOX1a $R^2=0,92$ $p < 0,05$. A statistically significant difference on the fit Ψ_w / RWC was found between Col-0 and AS-AOX1a plants ($p < 0,05$), but not in the fit Ψ_π / RWC.

A significant linear decrease of g_s with decreasing RWC ($p < 0,05$) was found for both AS-AOX1a and Col-0 (Fig. 5). A statistically significant difference was found for the slopes g_s / RWC between Col-0 and AS-AOX1a plants ($p < 0,05$). The mean g_s value of control AS-AOX1a plants ($1,02 \pm 0,47$ mol m⁻² s⁻¹) is significantly higher ($p < 0,05$) than the mean g_s values of control Col-0 plants ($0,40 \pm 0,23$ mol m⁻² s⁻¹). Under mild water stress, the mean g_s value for AS-AOX1a plants ($0,74 \pm 0,34$ mol m⁻² s⁻¹) is also significantly higher ($p < 0,05$).

than the mean g_s value of Col-0 ($0,28 \pm 0,16 \text{ mol m}^{-2} \text{ s}^{-1}$). No differences were found at moderate and severe water stress.

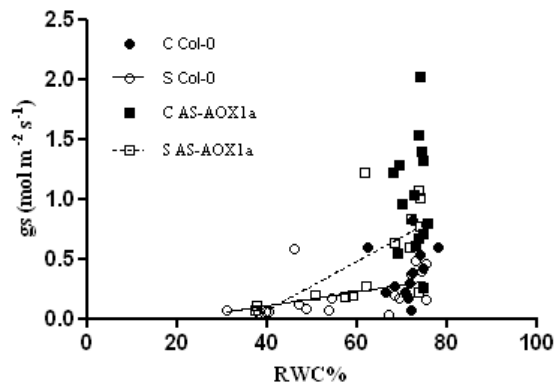


Fig. 5. Relation between g_s and RWC in Col-0 and AS-AOX1a plants under control and stress conditions. C – control; S – stress. Col-0: $r^2=0,245$ $p<0,05$; AS-AOX1a: $r^2=0,43$ $p=0,05$. A statistically significant difference on the slope g_s / RWC was found between Col-0 and AS-AOX1a plants ($p<0,05$).

3.2. Photosynthesis and photorespiration

3.2.1. A/C_c curves

In order to evaluate the photosynthetic performance of Col-0 and AS-AOX1a Arabidopsis plants subjected to water stress the A/C_c curves were constructed and V_{cmax} , J_{max} and TPU were determined and their evolution analyzed (Fig. 6).

In control Col-0 and AS-AOX1a plants the three photosynthetic parameters (Fig. 6) were not significantly different. The average values found in control Col-0 and AS-AOX1a plants were, respectively, 85.6 ± 18.0 and $81.5 \pm 11.1 \text{ } \mu\text{mol m}^{-2} \text{ s}^{-1}$ for V_{cmax} (Fig. 6A), 164.5 ± 33.5 and $156.6 \pm 15.0 \text{ } \mu\text{mol m}^{-2} \text{ s}^{-1}$ for J_{max} (Fig. 6B) and 14.4 ± 2.2 and $13.6 \pm 1.5 \text{ } \mu\text{mol m}^{-2} \text{ s}^{-1}$ for TPU (Fig. 6C).

In Col-0 and AS-AOX1a plants under stress conditions the variation of V_{cmax} , J_{max} and TPU with the leaf RWC was different. Whereas in Col-0 plants the three photosynthetic parameters linearly decreased with stress ($p<0.05$), no significant correlation was found between any of the photosynthetic parameters and RWC in AS-AOX1a plants.

No statistically significant differences were found between the slopes of Col-0 and AS-AOX1a fits for any of the photosynthetic parameters ($p<0.05$). However, it is possible to

observe that V_{cmax} in Col-0 plants (Fig. 6A) decreased more than in AS-AOX1a plants, which is reflected in the statistically significant differences found in severe water deficit ($31.3 \pm 5.1 \mu\text{mol m}^{-2} \text{s}^{-1}$ in Col-0 and $51.5 \pm 0.8 \mu\text{mol m}^{-2} \text{s}^{-1}$ in AS-AOX1a).

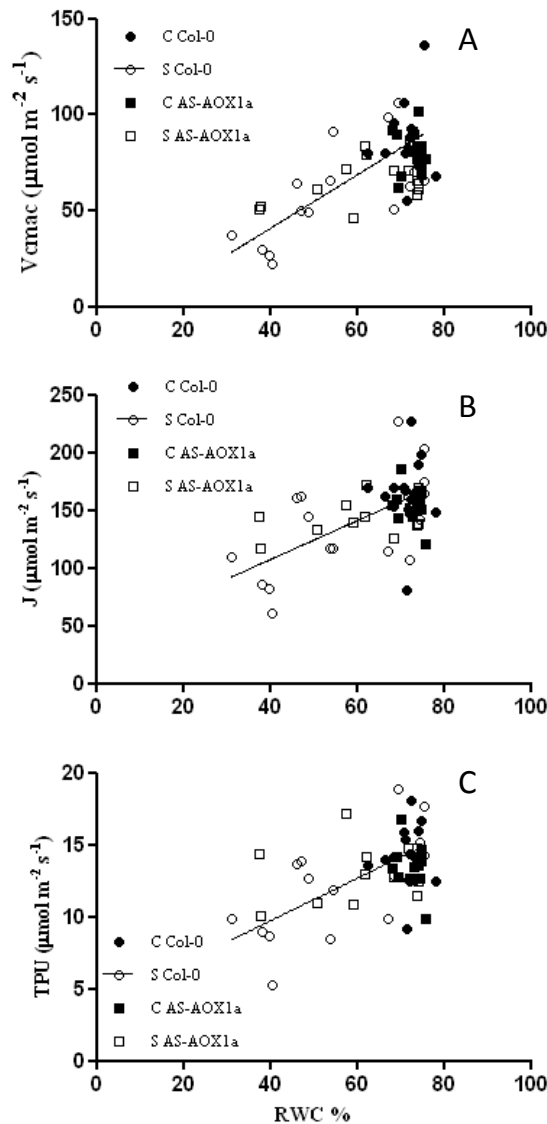


Fig. 6. Relation between V_{cmax} (A); J_{max} (B); TPU (C) and RWC in Col-0 and AS-AOX1a plants under control and stress conditions. C – control; S – stress. A: Col-0 $r^2=0,497$ $p<0,05$; AS-AOX1a $r^2=0,196$; $p>0,1$; B: Col-0 $r^2=0,374$ $p<0,05$ AS-AOX1a $r^2=0,2$; $p>0,1$; C: Col-0 $r^2=0,451$ $p<0,05$ AS-AOX1a $r^2=0,041$; $p>0,1$. No statistically significant differences were found between the slopes of Col-0 and AS-AOX1a for any of the three parameters ($p>0,05$).

A statistically significant linear decrease of A (Fig. 7A) with decreasing RWC was found for both Col-0 and AS-AOX1a ($p<0,05$), without statistically significant differences between the slope A / RWC of Col-0 and AS-AOX1a plants. The decrease of Phr with RWC was also significant, but whereas it was linear in Col-0, in AS-AOX1a it was quadratic. Thereby, a statistically significant difference between Phr / RWC of Col-0 and

AS-AOX1a plants was found. The decrease in Phr was lower than the decrease in A in Col-0 plants and thereby a significant quadratic increase in the ratio Phr/A ($p < 0.05$) with the decrease of RWC was found. In AS-AOX1a plants no correlation was found between the Phr/A ratio and RWC ($p > 0.05$) (Fig. 6C) due to a similar decrease of Phr and A with the RWC. Thereby, the slope (Phr/A) / RWC was significantly lower ($p < 0.05$) in AS-AOX1a than in Col-0 plants.

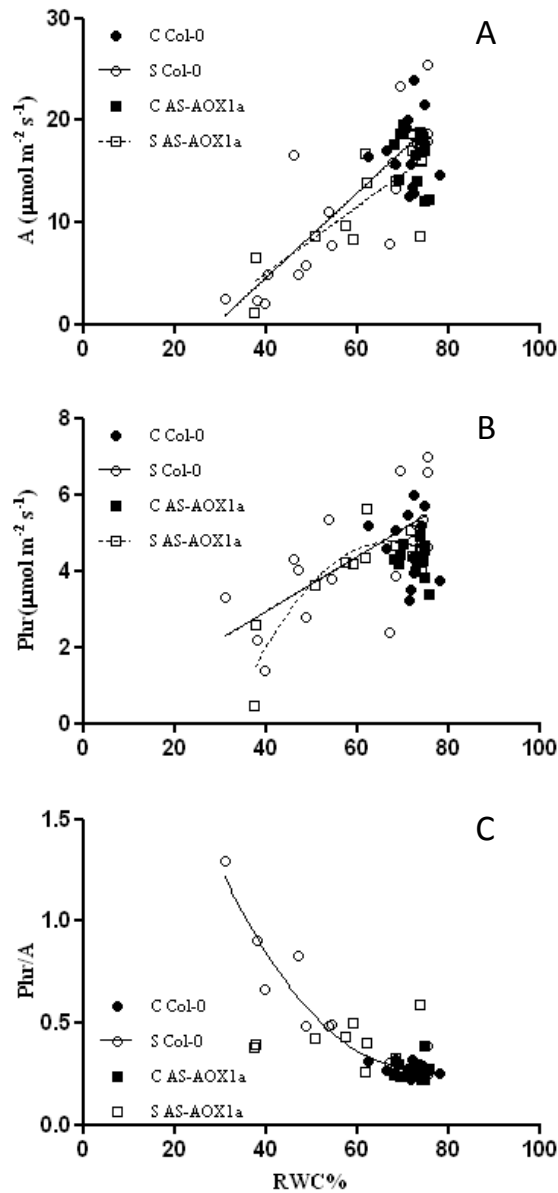


Fig. 7. Relation between A (A); Phr (B); Phr/A (C) and RWC in Col-0 and AS-AOX1a plants under control and stress conditions. C – control; S – stress. A: Col-0 $r^2=0,72$ $p < 0,05$; AS-AOX1a $r^2=0,661$ $p < 0,05$; B: Col-0 $r^2=0,47$ $p < 0,05$ AS-AOX1a $R^2=0,803$ $p < 0,05$; C: Col-0 $R^2=0,919$ $p < 0,05$ AS-AOX1a $r^2=0,1$ $p > 0,1$ A statistically significant difference between Col-0 and AS-AOX1a was only found for the slope Phr / RWC and Phr/A / RWC ($p < 0,05$).

3.2.2. *A/I curves*

Φ (Fig. 8A) and A_{max} (Fig. 8B) were linearly correlated with RWC in both Col-0 and AS-AOX1a plants ($p < 0.05$). No statistically significant difference was found between the Φ / RWC (Fig. 8A) and the A_{max} / RWC (Fig. 8B) slopes of Col-0 and AS-AOX1a plants ($p > 0.05$). LCP showed a statistically significant increase with decreasing RWC in both Col-0 and AS-AOX1a plants ($p < 0.05$) (Fig. 8C). The slope LCP / RWC was not significantly different between Col-0 and AS-AOX1a plants ($p > 0.05$). The mean LCP value for the Col-0 ($13.26 \pm 6.8 \mu\text{mol m}^{-2} \text{s}^{-1}$) was significantly higher than the one for the AS-AOX1a ($3.02 \pm 6.8 \mu\text{mol m}^{-2} \text{s}^{-1}$) plants in control conditions (Fig. 8C).

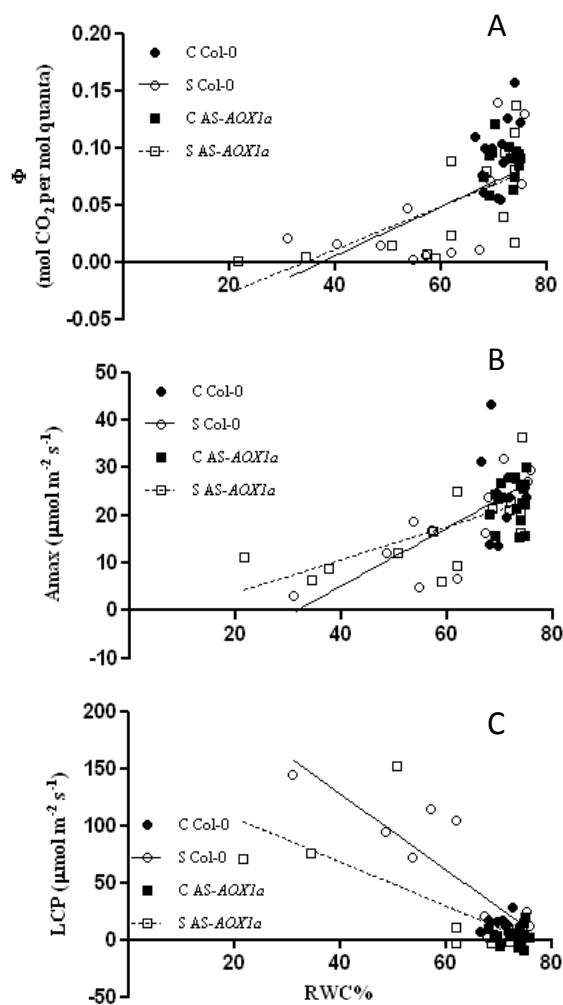


Fig. 8. A - Relation between Φ (A); A_{max} (B); LCP (C) and RWC in Col-0 and AS-AOX1a plants under control and stress conditions. C – control; S – stress. A: Col-0 $r^2=0,39$ $p < 0,05$ AS-AOX1a $r^2=0,416$ $p < 0,05$; B: Col-0 $r^2=0,642$ $p < 0,05$ AS-AOX1a $r^2=0,493$ $p < 0,05$; C: Col-0 $r^2=0,736$ $p < 0,05$ AS-AOX1a $r^2=0,476$ $p < 0,05$. No statistical difference between Col-0 and AS-AOX1a was found in any of the three parameters (for $p > 0,05$).

3.3. Chlorophyll a fluorescence

The chlorophyll a fluorescence was measured after dark adaptation and under two different light intensities: $200 \mu\text{mol m}^{-2} \text{s}^{-1}$ and $600 \mu\text{mol m}^{-2} \text{s}^{-1}$. F_0 , F_m and F_v/F_m (Fig. 9) were measured after 10 minutes in darkness. ETR, photochemical quenching (qP) and non-photochemical quenching (NPQ) were measured after 10 minutes in at $200 \mu\text{mol m}^{-2} \text{s}^{-1}$ followed by additional 10 minutes at $600 \mu\text{mol m}^{-2} \text{s}^{-1}$. F'_v/F'_m was calculated for each light regime (Fig. 10).

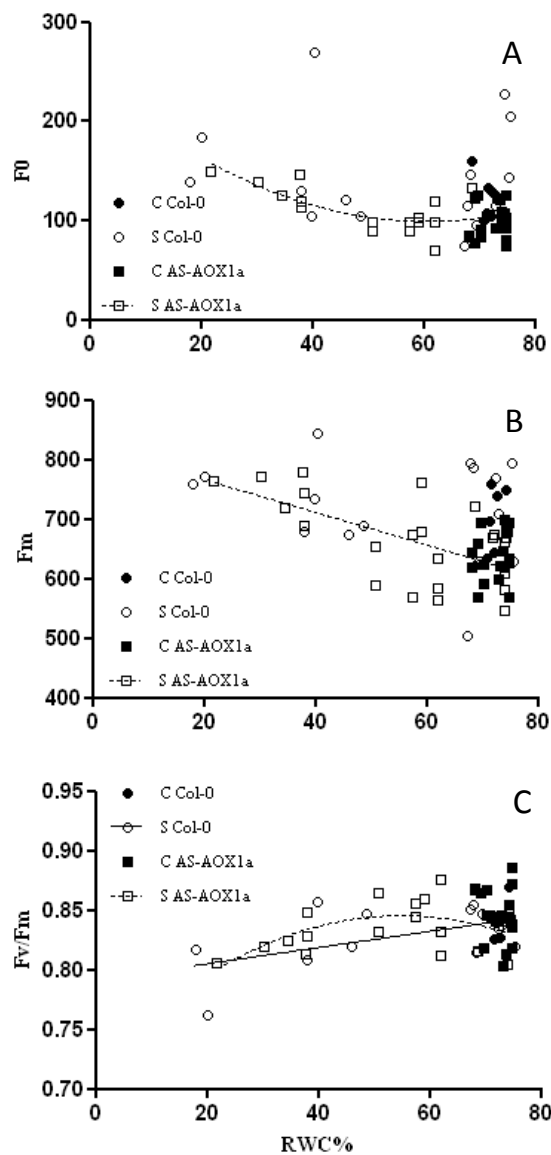


Fig. 9. Relation between F_0 (A); F_m (B); F_v/F_m (C) and RWC in Col-0 and AS-AOX1a plants under control (C) and stress (S) conditions. A: Col-0 $r^2=0,01$ $p>0,1$ AS-AOX1a $R^2=0,56$ $p<0,05$; B: Col-0 $r^2=0,062$ $p>0,1$ AS-AOX1a $r^2=0,390$ $p<0,05$; C:

Col-0 $r^2=0,283$ $p<0,1$ AS-AOX1a $R^2=0,289$ $p<0,1$. Statistical significant differences between Col-0 and AS-AOX1a plants were only found in Fo and Fv/Fm Vs RWC ($p<0,05$).

Whereas no significant correlation was found in Fo (Fig. 9A) and Fm (Fig. 9B) and RWC in Col-0 plants, a significant increase with decreasing RWC was found on AS-AOX1a plants ($p<0,05$). However, no differences in the slopes Fm / RWC were found between the two types of plants, in contrast with the relation Fo / RWC. Fv/Fm (Fig. 9C) showed a significant decrease with RWC for both types of plants ($p<0,1$), linear in the case of Col-0 and quadratic in AS-AOX1a. The variation Fv/Fm / RWC differ significantly between AS-AOX1a and Col-0 plants ($p<0,05$).

Whereas the ETR measured at $200 \mu\text{mol m}^{-2} \text{s}^{-1}$ does not significantly correlate with RWC in Col-0 plants ($p>0,05$) it does in AS-AOX1a plants where a statistically significant decrease of ETR was found with RWC ($p<0,05$) (Fig. 10A). The slope ETR / RWC at $200 \mu\text{mol m}^{-2} \text{s}^{-1}$ differ significantly between the two lines of plants ($p<0,05$). A significant decrease of ETR with decreasing RWC was found for both lines of Arabidopsis when the measurements were done at $600 \mu\text{mol m}^{-2} \text{s}^{-1}$ ($p<0,05$) (Fig. 10B). A statistically significant difference of the slope between Col-0 and AS-AOX1a plants was found at $600 \mu\text{mol m}^{-2} \text{s}^{-1}$. This is highlighted in Fig. 10B where control Col-0 plants showed mean ETR significantly higher ($124,4 \pm 3,0 \mu\text{mol m}^{-2} \text{s}^{-1}$) than the control AS-AOX1a plants ($119,3 \pm 3,6 \mu\text{mol m}^{-2} \text{s}^{-1}$) ($p<0,05$).

A statistically significant decrease of Fv'/Fm' with RWC was found when measured at both $200 \mu\text{mol m}^{-2} \text{s}^{-1}$ (Fig. 10C) and at $600 \mu\text{mol m}^{-2} \text{s}^{-1}$ (Fig. 10D), for both lines of Arabidopsis, with significant differences between the two lines in the slopes (Fv' / Fm') / RWC ($p<0,05$) only when measured at $600 \mu\text{mol m}^{-2} \text{s}^{-1}$.

A statistical significant correlation between qP and RWC was found for both Col-0 and AS-AOX1a plants ($p<0,05$) measured at $600 \mu\text{mol m}^{-2} \text{s}^{-1}$ PPFD (Fig. 10F) ($p<0,05$). Statistically significant differences on the slopes qP / RWC between Col-0 and AS-AOX1a, were found only when measured at $600 \mu\text{mol m}^{-2} \text{s}^{-1}$ PPFD. The qP of control Col-0 plants ($0,67 \pm 0,01$) was significantly higher than the qP of control AS-AOX1a plants ($0,63 \pm 0,02$) ($p<0,05$). No statistically correlation of NPQ with RWC was found for Col-0 and AS-AOX1a plants at $200 \mu\text{mol m}^{-2} \text{s}^{-1}$ ($p>0,05$) (Fig. 10G). Nevertheless, a statistically significant difference on the relation NPQ / RWC at $200 \mu\text{mol m}^{-2} \text{s}^{-1}$ between Col-0 and AS-AOX1a plants ($p<0,05$) (Fig. 10G) was found. At $600 \mu\text{mol m}^{-2} \text{s}^{-1}$ a statistically significant correlation between NPQ and RWC was only found for AS-AOX1a

plants, which showed a significant increase of NPQ with decreasing RWC ($p < 0,05$). A significant difference on the slope NPQ / RWC was found between Col-0 and AS-AOX1a, when measured at $600 \mu\text{mol m}^{-2} \text{s}^{-1}$ PPFD ($p < 0,05$) (Fig. 10H).

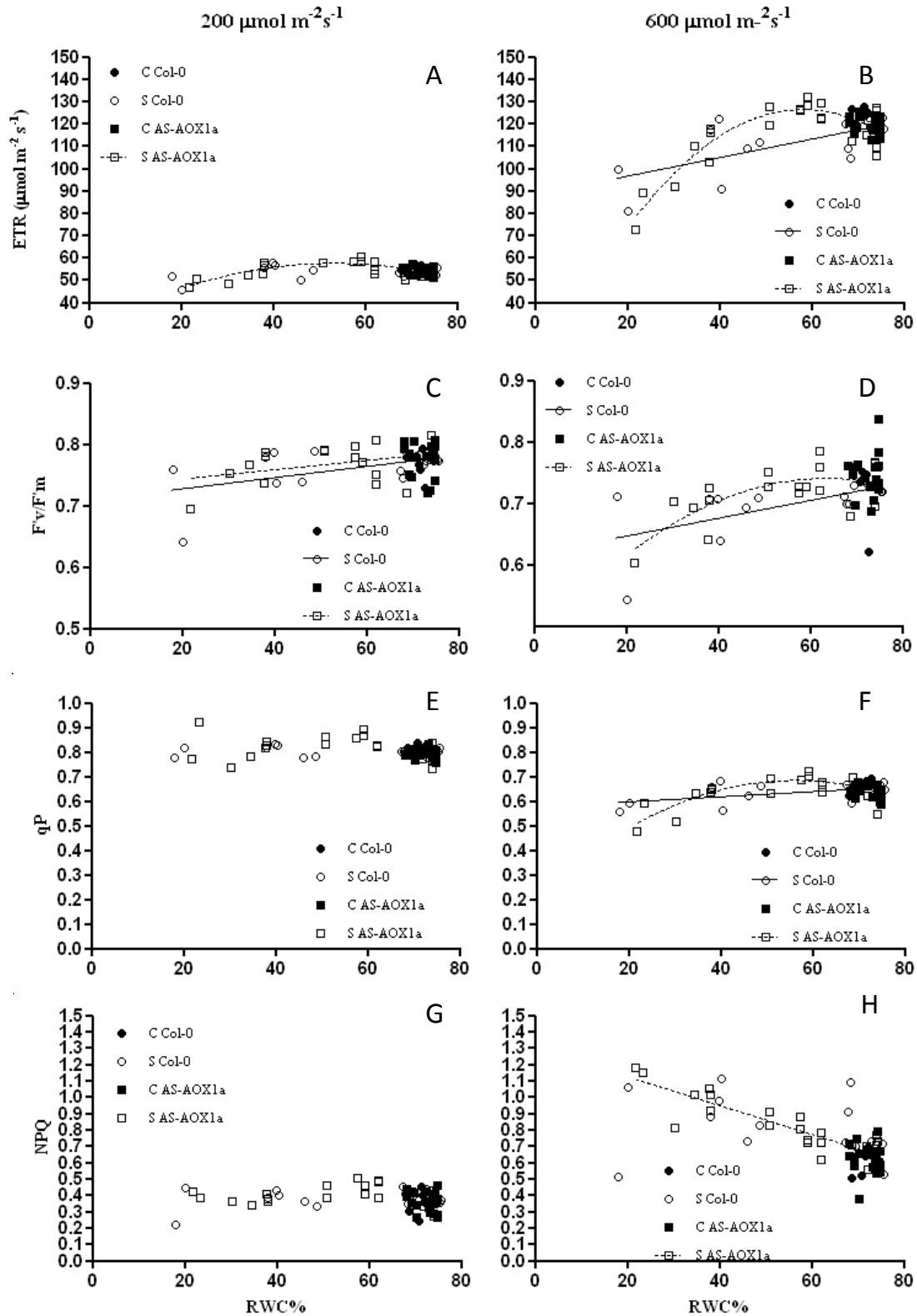


Fig. 10. Relation between ETR (A and B); F_v/F_m (C and D); qP (E and F); NPQ (G and H) with RWC at 200 μmol m⁻² s⁻¹ (A, C, E, G) and 600 μmol m⁻² s⁻¹ (B, D, F, H) in Col-0 and AS-AOX1a plants under control (C) and stress (S) conditions. A: Col-0 r²=0,091 p>0,1 AS-AOX1a R²=0,585 p<0,05; B: Col-0 r²=0,447 p<0,05 AS-AOX1a R²=0,815 p<0,05; C: Col-0 r²=0,251 p<0,05 AS-AOX1a r²=0,169 p<0,1; D: Col-0 r²=0,377 p<0,05 AS-AOX1a R²=0,528 p<0,05; E: Col-0 r²=0,002 p>0,1 AS-AOX1a r²=0,032 p>0,1; F: Col-0 r²=0,265 p<0,05 AS-AOX1a R²=0,626 p<0,05; G: Col-0 r²=0,084 p>0,1 AS-AOX1a R²=0,249 p>0,1; H: Col-0 r²=0,098 p>0,1 AS-AOX1a r²=0,788 p<0,05. Statistical significant differences on the relation F / RWC between the Col-0 and AS-AOX1a plants were found in ETR and NPQ at 200 μmol m⁻² s⁻¹ and ETR, F_v/F_m, qP and NPQ at 600 μmol m⁻² s⁻¹ (p<0,05).

3.4. Pigment quantification

Chlorophyll a (Ca), b (Cb) and total carotenoids (carotenes and xanthophylls (Cc+x)) were analyzed in both Col-0 and the AS-AOX1a Arabidopsis under control and stress conditions (Fig. 11).

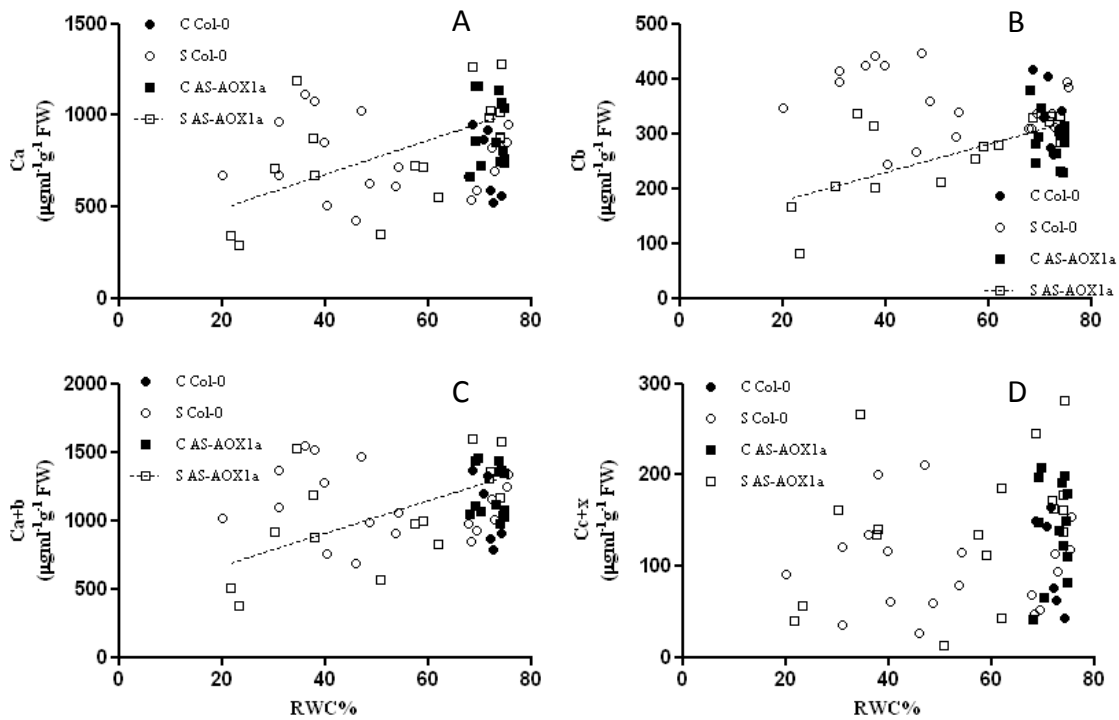


Fig. 11. Relation between Ca (A); Cb (B); Ca+b (C); Cc+x (D) and RWC in Col-0 and AS-AOX1a plants under control (C) and stress (S) conditions. A: Col-0 r²=0,02 p>0,1 AS-AOX1a r²=0,343 p<0,05; B: Col-0 r²=0,077 p>0,1 AS-AOX1a r²=0,497 p<0,05; C: Col-0 r²=0,033 p>0,1 AS-AOX1a r²=0,388 p<0,05; D: Col-0 r²=0,002 p>0,1 AS-AOX1a r²=0,142 p>0,1. Statistically significant differences between Col-0 and AS-AOX1a were found for the slopes Ca / RWC, Cb / RWC and Cc+x / RWC (p<0,05).

The decreases of Ca and Cb with decreasing RWC were statistically significant in AS-AOX1a plants, but no significant correlation was found between Ca and Cb and RWC in Col-0 plants (Fig. 11A and 11B). The slopes Ca / RWC and Cb / RWC in Col-0 were significantly lower than the corresponding slopes in AS-AOX1a plants ($p < 0,05$).

Also the total chlorophyll (Ca+b) significantly decreased with decreasing RWC in AS-AOX1a plants ($p < 0,05$) but no correlation between Ca+b and RWC was found in Col-0 plants (Fig. 11C). The slope Ca+b / RWC did not differ significantly between the two lines of plants.

No statistically significant correlation was found between Cc+x and RWC in any of the lines of plants. However, the slopes Cc+x / RWC significantly differ between Col-0 and AS-AOX1a (Fig. 11D).

Antocianins were not detected (data not shown).

3.5. Gene expression

In order to find the optimum number of cycles for each gene, allowing the visualization of PCR products in BET stained gels and preventing saturation, a RT-PCR was performed using as a template RNA from a severely-stressed Col-0 plant ($10\text{ng}/\mu\text{L}$). Samples corresponding to cycles 25, 30, 35, 40 and 40 plus a 10 min extension were analyzed by gel electrophoresis (Fig. 12).

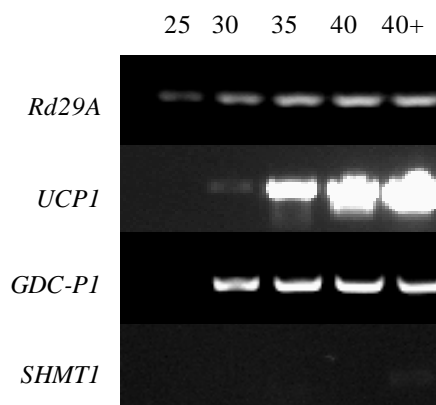


Fig. 12. RT-PCR products of *UCP1*, *RD29A*, *SHMT1* and *GDC-P1* genes after different PCR cycles in order to determinate the optimum numbers of cycles. Samples were taken at 25, 30, 35, 40 cycles and after the final extension, 40+. A severely-stressed RNA sample was used as template.

Fig. 12 shows that the transcripts of all the genes tested, except from *UCP2*, *UCP4* and *SHMT1*, could be amplified. The number of cycles to be used in subsequent analysis was 22 for *RD29A*, 28 for *UCP1* and 20 for *GDC-P1*.

The expression of *SHMT1* was tested on a control and on a severely-stressed RNA sample, 5 times concentrated (50ng/μL) with 45 PCR cycles (Fig. 13). Under these conditions it was possible to visualize the RT-PCR products in the control sample. For *UCP2* and *UCP4* no transcripts were detected even using RNA samples 10x concentrated (data not show). In view of this, the expression of these UCP genes was no further investigated.

A single band was observed for each primer pair and the correct sizes of the PCR products was checked accordingly to the preliminary bioinformatics analysis (Table 1) by co-migration with a DNA ladder (not shown). These results indicate that the design of the *RD29A* and *SHMT1* primers, made in the present work, was successful.

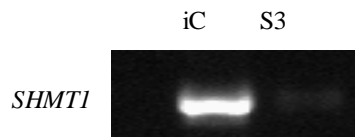


Fig. 13. RT-PCR performed with 45 cycles in order to determine the optimum number of cycles for *SHMT1*. iC, initial control; S3, severely-stressed Arabidopsis.

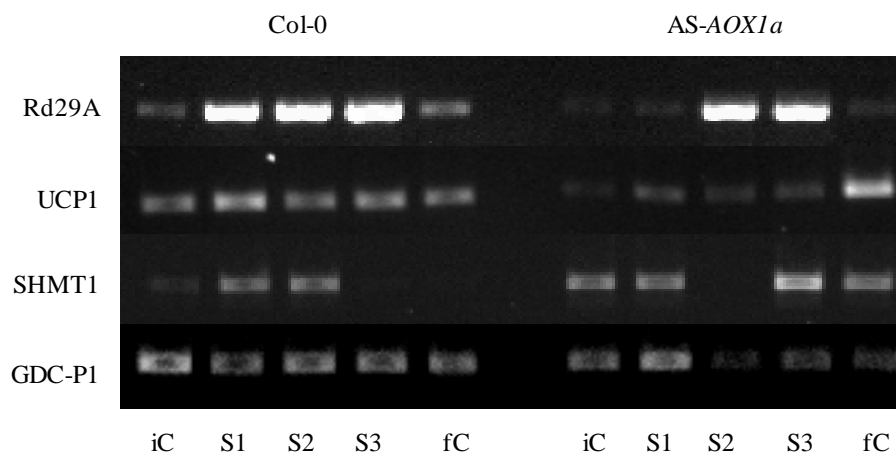


Fig. 14. RT-PCR products of *UCP1*, *RD29A*, *SHMT1* and *GDC-P* genes with the number of cycles previously determined and the respective T_m . Samples of 10ng/μL of RNA solution were used for *UCP1*, *RD29A* and *GDC-P1* genes. Samples of 50ng/μL of RNA solution were used on *SHMT1* gene. Col-0, wild type Arabidopsis; AS-AOX1a, transgenic Arabidopsis; iC, initial control; S1 mild Stress Arabidopsis; S2 moderate Stress Arabidopsis; S3, severe Stress Arabidopsis; fC, final Control.

Gene expression was analyzed in RNA samples from Col-0 and AS-AOX1a plants (Fig. 14). Controls from the beginning (iC) and the end (fC) of the experimental period were analyzed to account for possible developmental changes on the expression of the genes under study. The purity of all the RNA samples was verified by spectrophotometry and the integrity and concentrations of the working solutions was verified by gel electrophoresis (data not shown). In addition the expression of a housekeeping gene encoding a ribosomal protein (*S24*) was shown to display a constitutive expression on these RNA samples (D. Pinxteren and A.R. Matos, personal communication).

As expected, the expression of *RD29A* was up-regulated in stressed plants compared to both controls (Fig.14). The up-regulation of this gene can be already observed in S1 WT plants, which had RWCs similar to those found in control plants, confirming that this gene is a suitable molecular marker for the early drought-stress response, in our experimental system.

The *UCP1* gene showed an almost constitutive expression in Col-0 plants, with a slightly more pronounced expression in S1. In the AS-AOX1a Arabidopsis, *UCP1* displayed a similar increase at S1, however the overall expression levels were lower in AS-AOX1a plants, with the exception of fC plants (Fig. 14). Lower expression levels were also observed for the majority of the AS samples for *GDC-P1*. The expression of this gene tends to decrease with water deficit, with the exception of AS-AOX1a plants at S1. In both genotypes, the controls of the end of the experiments have less *GDC-P1* transcripts than the controls collected at the beginning.

In Col-0 well-watered plants *SHMT1* is very little expressed. Its expression is up-regulated by drought at S1 and S2 and the amounts of this mRNA return to control levels in severely-stressed plants (Fig. 14). Well-watered transgenic plants express *SHMT1* gene at higher levels than Col-0 and transcript levels remain high at S1 with an increase at S3 (Fig. 14). The apparent lack of transcripts in S2 plants, as well as the other results above presented, should be further confirmed in replicate experiments with other RNA series, which were not carried out in the present work due to time limitations.

4. Discussion

4.1. Water relations

RWC, Ψ_w and g_s were screened to select the parameter that better describes the water status of *Arabidopsis* leaves. Although g_s has been successfully used in other works to monitor water deficit (Nunes et al., 2008), we found that in *Arabidopsis* the relation between A and g_s is not linear. In fact, although A and g_s (Fig. 1B) are highly correlated ($R^2=0,869$), for a wide range of g_s (1.5 to 0.5 mol m⁻² s⁻¹) photosynthesis does not change significantly and only for g_s values lower than 0.5 mol m⁻² s⁻¹ there is a marked decrease of A.

On the other hand, the worst correlation with A was found for Ψ_w (Fig. 1C) which was discarded as a suitable indicator of water stress in *Arabidopsis* leaves.

On the contrary, the relation between A and RWC ($r^2 = 0.72$) shows a high correlation and furthermore has the practical and theoretical advantage of being linear (Fig. 1A). Therefore, RWC seems to be the most suitable parameter to express *Arabidopsis* water status. However, even if results are to be expressed in a RWC basis, neither g_s nor Ψ_w should be discarded as these parameters also provide important information about the plant water status.

The phenotype of *Arabidopsis* under normal growth conditions was the same for Col-0 and AS-AOX1a plants, as previously observed (Fiorani et al., 2005; Watanabe et al., 2008; Giraud et al., 2008; Strodtkötter et al. (2009). It is worth to note that as the duration of the stress period was 14 days, at the end of the experiment control plants were two weeks older than at the beginning, which explains the difference in plant size that can be observed in Fig. 2.

The plants subjected to mild stress showed RWC similar to the controls (Fig. 2). Stress responses may be elicited before any decrease of leaf RWC occurs. Plant roots have stress sensors that may react to early changes in SWC leading to the synthesis of ABA, which may cause stomatal closure in leaves (Shinozaki and Yamagushi-Shinozaki, 1997). In fact, it was possible to observe that at SWC higher than 30-40% most stressed plants could kept their RWC at the control values. Nonetheless, stress was already sensed, as shown by the up-regulation of *RD29A* (a drought induced gene) at S1 in the Col-0 plants.

SLA values in stress are lower than the values of control plants, indicating that stressed leaves became denser, which suggests that in prolonged or severe drought leaf structural alterations may arise both in the wild type and the transgenic plants. The results also suggests that the structural alterations proceeds faster in Col-0 plants, as at S1 their SLA was significantly lower than the SLA of AS-AOX1a plants, but this result needs further confirmation.

Although both Col-0 and AS-AOX1a plants display the same behavior with the decrease of RWC, the Col-0 always had higher Ψ_w than AS-AOX1a for the same RWC. Although the Col-0 plants showed higher values ($-0,37 \pm 0,11$ MPa) of Ψ_{π} in control conditions than AS-AOX1a plants ($-0,47 \pm 0,06$ MPa), no overall significant differences were found between the two lines in Ψ_{π} , suggesting that the lower overall Ψ_w of AS-AOX1a is probably due, at least in part, to a lower pressure potencial, suggesting less elastic cell walls in the AS plants. It has been previously observed that elastic cell walls are associated with a high desiccation tolerance (Fan et al., 1994). One possible hypothesis is that Col-0 plants are able to display a more elastic cell wall than the AS-AOX1a plants, which allows them to better resist drought stress. On the other hand, the lower values of Ψ_{π} in the AS-AOX1a plants under control conditions indicates that these plants had a higher concentration of cell solutes than the Col-0 plants for those conditions, partly responsible for their lower Ψ_w . Two mechanism can be envisaged for the need of lower Ψ_w in AS plants to attain the some RWC of Col-0 plants: a) AS plants have a lower hydraulic conductivity, demanding a higher water potential gradient between the leaves and the soil; or b) AS plants have a higher stomatal conductance, demanding a higher water uptake rate to replenish the water lost by transpiration. In fact, the stomatal conductance of control AS-AOX1a plants is much higher than in Col-0 plants (Fig. 5), supporting the second hypothesis.

Despite The high variability of g_s values (Fig. 5) it was still possible to observe a significant correlation between this parameter and RWC on Col-0 and AS-AOX1a plants. g_s values for Col-0 were lower under control and mild stress conditions, meaning that Col-0 plants have a higher resistance to gas diffusion in those conditions. The AS-AOX1a plants only displayed the same level of resistance to gas diffusion for moderate and severe stress. This could mean Col-0 plants are sensing drought at higher RWCs than AS-AOX1a plants and therefore probably promoting ABA synthesis leading to stomatal closure.

4.2. Photosynthesis and photorespiration

4.2.1. A/C_c curves,

The response of net photosynthesis to different concentrations of C_c describes two, sometimes three, distinct phases (Farquhar et al., 1980; von Caemmerer, 2000). When C_c starts to get higher from its minimal concentration the slope A/C_c is high and it is determined by the maximum Rubisco carboxylation rate, i.e. the V_{cmax} . While the CO_2 concentration increases, the slope of the curve decreases, sometimes getting close to zero due to limitations related with the regeneration of RuBP. At a saturating irradiance this is the maximum rate of electron transport driving regeneration of RuBP, the J_{max} . Sometimes a third phase can be seen with a slope of zero or lower if the rate of the use of triose phosphate, the TPU, becomes limiting. The first two phases were mathematically described by Farquhar et al. (1980) and modified, to include the third phase, by von Caemmerer (2000). Normally only the two first phases occur because the use of triose phosphate does not become limiting (Long and Bernacchi, 2003). The model of Farquhar et al. (1980) was developed taking in account the chloroplast metabolism but due to the difficulty to estimate C_c and the small difference between C_i and C_c found in some species it was frequent to fitting an A/C_i curve instead of an A/C_c curve. However, CO_2 needs to diffuse from the sub-stomatic chamber to the intercellular spaces, go through mesophyll cell walls, plasmatic membranes and chloroplast membranes. It was found that this trajectory comprises resistance to CO_2 transport and consequently, a significant difference between C_i and C_c in most species (von Caemmerer, 2000). Taking into consideration the mesophyll conductance (g_m) to CO_2 diffusion and the concomitant transformation of C_i to C_c , leads to significant modifications in the curve A/C_c , mainly to its curvature which is quite relevant in V_{cmax} determination (Sharkey et al., 2007).

In some species, when A decreases with the initial decrease of RWC, rising the external level of CO_2 (C_{ext}) from 5 to 15% restores the initial value of A (Cornic, 2000). Below a critical RWC, however, A keeps decreasing and high values of C_{ext} are not enough anymore to restore its initial value, revealing, then, the occurrence of metabolic limitations at low RWC. This type of response is called a type 1 limitation (Lawlor and Cornic, 2002). In other species, A decreases progressively with RWC and is less stimulated by the increase in C_{ext} which shows that the g_s effect is less important than metabolic limitations since the onset of stress. It is a type 2 response (Lawlor and Cornic, 2002).

In this work, the parameters obtained from the A/C_c curves show a limitation either by damage or metabolic adjustments that contributes to the decrease of A . V_{cmax} decreases significantly in Col-0 plants with the drop of RWC, while in AS-AOX1a the observed decrease was not statistically significant. Furthermore, under severe stress the mean V_{cmax} value of Col-0 was significantly lower than the corresponding value of AS-AOX1a. This might have happen because Col-0 plants are being more limited at the Rubisco carboxylation site than AS-AOX1a plants, for this level of stress. Although drops in V_{cmax} were already reported in Col-0 Arabidopsis under drought and other stresses (Poulson et al., 2006; Flexas et al., 2007) and also in other species (Lal et al., 1996; Nunes et al., 2008) no information was found regarding the behavior of V_{cmax} in *AOX1a* mutants.

J_{max} and TPU decreased significantly with the onset of drought stress in Col-0 but no significant correlation of these parameters with RWC was found in AS-AOX1a plants. Nevertheless, these results do not permit to conclude if these plants have different physiological behaviors when in drought stress. Decreases in J_{max} with water stress were previously described in other plants (Sharkey and Seeman, 1988; Nunes et al., 2008). No records of TPU variation were found for Arabidopsis, however for other plant species it was observed that TPU can become a limiting factor for photosynthesis (Maroco et al., 2002; Díaz-Espejo et al., 2006).

Although the slopes of A / RWC were similar in Col-O and AS-AOX1a, the slopes of Phr / RWC were not, and therefore when the ratio Phr/A was analyzed statistically significant differences were found; the increase of Phr / A was statistically significant in Col-0 ($p < 0.05$) but not in AS-AOX1a. Whereas in Col-0 plants the decrease of A was more pronounced than the decrease of Phr , in AS-AOX plants the opposite situation was found suggesting that the lack of *AOX1a* is in fact compromising the photorespiration of AS-AOX1a Arabidopsis.

4.2.2. *A/I* curves

No significant differences between the slopes of Col-0 and AS-AOX1a plants were found for A_{max} , Φ and LCP with decreasing RWC. A_{max} declined with water stress due to a lower stomatal conductance that limited the carboxylation capacity of the Calvin cycle. Also, a limitation on carbon fixation could result from light energy dissipation in other metabolic processes. Of the several processes involving light energy dissipation (*e. g.* Mehler-ascorbate peroxidase reactions) only photorespiration could significantly alter

carbon fixation (Long et al., 1994). Also the decrease in Φ with decreasing RWC suggests an increase in photorespiration at low irradiance. However it is interesting pointing out that under moderate stress both types of plants displayed a reduction of 50% of the A_{max} control value, whereas the decrease of Φ was even bigger, around 90%, suggesting strong limitations at the photosynthetic electron transport chain. The LCP increased with the decrease of RWC for both types of plants should result from a higher photorespiration rate since respiration didn't changed significantly (results not shown). The higher photorespiration rate can be related to the decrease of Rubisco carboxylase activity proportionally to the oxigenase activity under water stress due to a lower CO_2/O_2 ratio. It has been stated that the increase in LCP might be also related to an increase of Rubisco inhibitors that are formed with light conditions (Kane et al., 1998). These inhibitors can be involved in the protection of Rubisco under stress conditions avoiding its degradation (Parry et al., 2002). It is remarkable that in control conditions Col-0 plants displayed LCP values much higher than AS-AOX1a plants. Any of discussed mechanisms may explain this difference in the control plants, but it is tempting to attribute it to a lower photorespiration of the AS-AOX1a plants.

4.3. Chlorophyll a fluorescence

When observing the results from fluorescence measured in dark-adapted leaves, it was possible to see that F_o increased with the onset of stress in AS-AOX1a plants. It was also possible to detect, in AS-AOX1a plants a slight increase in the maximum fluorescence level suggesting that the cause of the increase might have been due to an higher chlorophyll content. However, this hypothesis is not supported by the notorious decrease of chlorophyll content found on AS-AOX1a plants (Fig. 11). It must be noted, however, that the relation between basal fluorescence and the chlorophyll content is not linear: F_o increases with the chlorophyll content initially and then decrease due to fluorescence reabsorption at high chlorophyll concentrations. Therefore, an effect of chlorophyll content on the observed variation of F_o and F_m is not to exclude. A significant difference on F_v/F_m between the Col-0 and AS-AOX1a plants was found with a significant curvilinear decrease with RWC in AS-AOX1a plants and a significant linear decrease in Col-0 plants, indicating that the maximal potential quantum efficiency of PSII is being affected by stress in both lines of plants. However, it must be strengthened that the absolute decrease on F_v/F_m values was very small, as for RWC as low as 20% F_v/F_m values above 0,8 were still found. Although the function of PSII reaction centre is known to be remarkably

resistente to water stress (Genty et al., 1989), these results suggest an exceptional resistance in *Arabidopsis*.

Significant differences were found between the Col-0 and AS-AOX1a *Arabidopsis* for ETR and NPQ at 200 $\mu\text{mol m}^{-2} \text{s}^{-1}$ and ETR, $F'v/F'm$, qP and NPQ at 600 $\mu\text{mol m}^{-2} \text{s}^{-1}$. It was possible to observe, in AS-AOX1a plants, a very small decrease ETR values at 200 $\mu\text{mol m}^{-2} \text{s}^{-1}$ but not for Col-0 plants at 200 $\mu\text{mol m}^{-2} \text{s}^{-1}$. This means that AS-AOX1a plants showed a limitation in the electron transport rate through PSII. At 600 $\mu\text{mol m}^{-2} \text{s}^{-1}$, differences between the two lines of plants were visible, but the ETR decrease was observed more clearly. When qP at 600 $\mu\text{mol m}^{-2} \text{s}^{-1}$ was analyzed it was possible to observe a slight decrease for both the Col-0 and AS-AOX1a plants. This decrease of both ETR and qP means that the quinone pool have become more reduced due limitations downstream, possible in the Calvin cycle. After analyzing the NPQ, statistical differences were found between the two sets of plants at 600 $\mu\text{mol m}^{-2} \text{s}^{-1}$, as AS-AOX1a NPQ tended to increase more than Col-0 plants in severe stress, which would be in agreement with the results of Giraud et al. (2008). This overall increase of NPQ can be explained by a decrease in the rate of consumption of NADPH and ATP which can result from several restrictions (Baker and Rosenqvist, 2004). Such restrictions imposed on PSII electron transport can lead to an increase in the proton electrochemical potential difference across the thylakoid membrane. These results in an increase in non-photochemical quenching in the PSII antennae, which will be detected by an increase in NPQ and a decrease in $F'v/F'm$ (Baker and Rosenqvist, 2004) which was also observed.

4.4. Pigment quantification

It is known that drought stress decreases the amount of chlorophyll a and b as a result of the degradation of the chloroplast structure ending in pigment leak (Ristic and Cass, 1991). This decrease was visible in chlorophyll a and b and only in the AS-AOX1a *Arabidopsis* with statistical significance. .

4.5. Gene expression

The RD29A has a promoter with a repeated sequence termed dehydration-responsive element (DRE), and is thus up-regulated in the initial rapid response to drought, salt or low

temperature stresses (Ingram and Bartels, 1996). This gene was studied in the present work as a “marker” to detect the effects of drought at the transcriptional level and thus, provide further information concerning the first effects of this stress, which occur before changes in other physiological indications of water deficit, such as the RWC, Ψ_w or g_s . It was possible to observe that in Col-0 plants, the gene was poorly expressed in the controls, whereas in the three stages of stress it showed a strong increase in expression. This observation allows identifying limiting SWC values that Arabidopsis perceives as stressful and will be extremely useful in choosing the samples to be analyzed in future works with the same genotypes. The fact that *RD29A* expression remained lower in AS-AOX1a could indicate a delayed stress signaling mechanism, which would be in agreement with the higher g_s values observed in the transgenic line. Indeed, in Arabidopsis plants overexpressing a lipase gene, which conferred increased drought tolerance, the expression of *RD29A* was shown to be more rapid and more intense after an osmotic stress treatment (Hong et al., 2008). However, our results require further confirmation by replicate experiments.

Since UCP, as AOX, contributes to mitochondrial energy dissipation as heat, both proteins could have similar physiological roles. In a recent study it has been shown that an insertional knockout, lacking *UCP1* transcripts, displayed restrictions in photorespiration with a decrease in the rate of oxidation of photorespiratory glycine, leading to an associated reduced photosynthetic carbon assimilation rate (Sweetlove et al., 2005). Our results also point to an impaired photorespiratory metabolism in AS-AOX1a plants suggesting that both proteins are important in photorespiration. Here we have observed a decreased expression of *UCP1* in AS-AOX1a plants indicating that UCP is not compensating for the lack of AOX. Interestingly, the T-DNA *UCP1* mutants also had reduced AOX protein contents compared to the WT plants (Sweetlove et al., 2006). The absence of *UCP2* and *UCP4* expression is in agreement with previous studies showing that *UCP2* and *UCP4* show far less expression than *UCP1*. *UCP2* is mainly expressed in the roots (Hourton-Cabassa et al., 2004).

GDC is a protein complex composed of four proteins including the *P* protein which is the actual glycine decarboxylating subunit and is encoded by two genes in Arabidopsis (Bauwe and Klukisaoglu, 2003; Engel et al., 2007). Although our study does not provides information on the amounts of the GDC protein complex present in mitochondria, the analysis of *GDC-P1* transcripts indicates if a transcriptional limitation is being caused by the stress or the mutation under study. It is noteworthy that there is a reduction in the expression of *GDC-P1* gene in the WT at the onset of the drought response (S1) that

parallels the decrease in photorespiration suggested by gas-exchange analysis. Accordingly, the overall decreased expression of this gene in AS-AOX1a plants, compared to the Col-0 would be in agreement with an impairment in photorespiration in this line.

SHMT is encoded by seven genes in Arabidopsis, but only two have mitochondrial targeting sequences. We have selected for our study the gene encoding the major isoform present in Arabidopsis leaves (Voll et al., 2006). In contrast to *GDC-P1*, *SHMT1* gene is up-regulated by drought stress in Col-0 plants, suggesting a possible compensation for the decrease in *GDC* expression. Similarly AS-AOX1a plants which have lower amounts of *GDC-P1* transcripts have increased amounts of *SHMT1* mRNA.

5. Conclusions

No morphological differences were visible either in control or stress condition between the two lines of *Arabidopsis* used in this study (AS-AOX1a and Col-0) as shown by the photographs. However, a delayed drought-induced decrease of SLA was observed for the AS-AOX1a.

The plants in mild water stress displayed similar RWC to those found in control plants but, as was shown by *RD29A* expression, a water deficit response had already been triggered at this stage of the drought stress.

AS-AOX1a plants displayed lower water potential values for the same RWC as Col-0 plants which might indicate a less tolerance to drought stress. Also in control plants it was visible lower values of osmotic potential in AS-AOX1a plants suggesting a higher solute concentration.

It was also observed higher stomatal conductance values in AS-AOX1a under control and mild water stress plants which might point to a diminished capacity to sense drought and therefore dealing ABA synthesis and consequently stomatal closure.

Photosynthetic parameters have shown limitations due water deficit. The maximum rate of Rubisco carboxylation showed a significant decrease in Col-0 plants that was not visible in AS-AOX1a plants. In severe stress the difference between the two types of plants in this parameter was very high which indicates these plants shows bigger limitation in the Rubisco carboxylation site for severe stress.

It was also visible a decrease in photorespiration in both Col-0 and AS-AOX1a plants but with the transgenic plants reaching lower values. This bigger decrease of photorespiration in AS-AOX1a plants was reflected in the ratio photorespiration / photosynthesis. It was also observed a decrease in photosynthesis at maximum irradiance and in quantum yield of PSII electron transport in both lines of plants. It was found an increase in the light compensation point for both Col-0 and AS-AOX1a but higher in Col-0 plants which suggests a higher photorespiratory rate in those plants opposing to AS-AOX1a plants.

AS-AOX1a plants displayed increasing values of F_o and F_m related to a higher chlorophyll content, however when the chlorophyll content was measured it was possible to observe a decrease of C_a and C_b in AS-AOX1a plants but not for Col-0 plants.

It was visible, in both AS-AOX1a and Col-0 a decrease of ETR and qP showing a bigger reduction in plastoquinone pool. Also visible was a higher NPQ in AS-AOX1a in severe stress.

Gene expression showed lowered expression of *GDC-P1* in AS-AOX1a in agreement with possible limitation in the photorespiration rate. A similar behavior was observed for *UCP1* recently suggested to be necessary to a optimum photosynthesis. The higher expression of *SHMT1* in AS-AOX1a on the other hand seems to point to a compensatory effect.

All the parameters studied seem to indicate that the lower expression of *AOX1a* had an impact on the physiology of the AS-AOX1a plants. Some of the differences are visible in control conditions and many others are observed in response to drought stress. Together the results suggest that the AS-AOX1a by displaying lower expression of *AOX1a* is affected in photorespiration and that impairment gets reflected in photosynthetic metabolism.

6. References

- Andersson M., Nordlund P. 1999. A revised model of the active site of alternative oxidase. *Federation of European Biochemical Societies Letters* **449**: 17-22.
- Aranha A., Matos A.R, Mendes A., Vaz-Pinto V., Rodrigues C., Arrabaça J. 2006. Dinitro-o-cresol induces apoptosis like cell death but not alternative oxidase expression on soybean cells. *Journal of Plant Physiology* **164**: 675-84.
- Atkin O., Macherel D. 2009. The crucial role of plant mitochondria in orchestrating drought tolerance. *Annals of Botany* **103**: 581-597.
- Baker N., Rosenqvist E. 2004. Applications of chlorophyll fluorescence can improve crop production strategies: an examination of future possibilities. *Journal of Experimental Botany* **55**: 1607-1621.
- Bauwe H., Kolukisaoglu Ü. 2003. Genetic manipulation of glycine decarboxylation. *Journal of Experimental Botany* **54**: 1523–1535.
- Borecký J., Nogueira F., Oliveira K., Maia I., Vercesi A., Arruda P. 2006. The plant energy-dissipating mitochondrial systems: depicting the genomic structure and the expression profiles of the gene families of uncoupling protein and alternative oxidase in monocots and dicots. *Journal of Experimental Botany* **57**: 849–864.
- Brandalise M., Maia I., Borecký J., Vercesi A., Arruda P. 2003. Overexpression of plant uncoupling mitochondrial protein in transgenic tobacco increases tolerance to oxidative stress. *Journal of Bioenergetics and Biomembranes* **35**: 203-209.
- Catsky J. 1960. Determination of water deficit in discs cut out from leaf blades. *Biologia Plantarum* **2**: 76-77.
- Clifton R., Lister R., Parker KL., Sappl PG., Elhafez D., Millar AH., Day D., Whelan J. 2005. Stress-induced co-expression of alternative respiratory chain components in *Arabidopsis thaliana*. *Plant Molecular Biology* **58**: 193-212.

Coombs J., Hall D., Long S., Scurlock J. 1987. Techniques in bioproductivity and photosynthesis. Pergamon Press, Oxford.

Cornic G. 2000. Drought stress inhibits photosynthesis by decreasing stomatal aperture – not by affecting ATP synthesis. *Trends in Plant Science* **5**: 187-188.

Costa J., Jolivet Y., Hasenfratz-Sauder M., Orellano E., da Guia Silva Lima M., Dizengremel P., Fernandes de Melo D. 2007. Alternative Oxidase regulation in roots of *Vigna unguiculata* cultivars differing in drought/salt tolerance. *Journal of Plant Physiology* **164**: 718-27.

Daniel, W.D. (1987). Biostatistics: A foundation for analysis in the health sciences. John Wiley & Sons, New York.

Días-Espejo A., Walcroft A., Fernández J., Hafidi B., Palomo M., Girón I. 2006. Modeling photosynthesis in olive leaves under drought conditions. *Tree Physiology* **26**: 1445–1456.

Douce R., Bourguignon J, Neuburger M, Rebeille F. 2001. The glycine decarboxylase system: a fascinating complex. *Trends in Plant Science* **6**: 167–176.

Engel N., Daele K., Kolukisaoglu U., Morgenthal K., Weckwerth W., Pärnik T., Keerberg O., Bauwe H. 2007. Deletion of glycine decarboxylase in *Arabidopsis* is lethal under nonphotorespiratory conditions. *Plant Physiology* **144**: 1328– 1335.

Fan S., Sharkey T., Berry J., Farquhar G. 1994. The relative contribution of elastic and osmotic adjustments to turgor maintenance in woody species. *Physiologia Plantarum* **90**: 408-413.

Farquhar G., von Caemmerer S. Berry J. 1980. A biochemical model of photosynthetic CO₂ assimilation in leaves of C3 species. *Planta* **149**: 78-90.

Fiorani F., Umbach A.L., Siedow J.N. 2005. The alternative oxidase of plant mitochondria is involved in the acclimation of shoot growth at low temperature. A study of *Arabidopsis aox1a* transgenic plants. *Plant Physiology* **139**: 1795–1805.

Flavell R. 2009. Role of Model Plant Species. *Methods in Molecular Biology* **513**: 1-18

Flexas J., Ortuño M., Ribas-Carbo M., Diaz-Espejo A., Flórez-Sarasa I., Medrano H. 2007. Mesophyll conductance to CO₂ in *Arabidopsis thaliana*. *New phytologist* **175**: 501-511.

- Genty B., Briantais J., Baker N. 1989. The relationship between the quantum yield of photosynthesis electron transport and quenching of chlorophyll fluorescence. *Biochemical. Biophysical Acta* **990**: 87-92
- Giraud E., Ho L., Clifton R., Carroll A., Estavillo G., Tan Y., Howell K., Ivanova A., Pogson B., Millar A., Whelan J. 2008. The absence of Alternative Oxidase 1a in *Arabidopsis thaliana* results in acute sensitivity to combined light and drought stress. *Plant Physiology* **147**: 595-610.
- Havaux M. 1998. Carotenoids as membrane stabilizers in chloroplasts. *Trends in Plant Science* **3**: 147-151
- Hoefnagel M., Millar A., Wiskitch J., Day D. 1995. Cytochrome and alternative respiratory pathways compete for electrons in the presence of pyruvate in soybean mitochondria. *Archives of Biochemistry and Biophysics* **318**: 394-400.
- Hong J.K., Choi H.W., Hwang I.S., Kim D.S., Kim N.H., Choi D.S., Kim Y.J., Hwang B.K. 2008. Function of a novel GDSL-type pepper lipase gene, CaGLIP1 in disease susceptibility and abiotic stress tolerance. *Planta* **227**: 539-558.
- Hopkins W. 1999. Introduction to Plant Physiology, 2nd edition. John Wiley & Sons, Inc. Chapter 10: 189-190.
- Hourton-Cabassa C., Mato A.R., Zachowski A., Moreau F. 2004. The plant uncoupling protein homologues: a new family of energy-dissipating proteins in plant mitochondria. *Plant Physiology and Biochemistry* **42**: 283-290.
- Igamberdiev A., Bykova N., Gardeström P. 1997. Involvement of cyanide resistant and rotenone insensitive pathways during oxidation of glycine in higher plants. *Federation of European Biochemical Societies Letters* **412**: 265–269
- Igamberdieva A., Bykova N., Leab P., Gardeström P. 2001. The role of photorespiration in redox and energy balance of photosynthetic plant cells: a study with a barley mutant deficient in glycine decarboxylase. *Physiologia Plantarum* **111**: 427–438.
- Ingram J., Bartels D. 1996. The molecular basis of dehydration tolerance in plants. *Annual Review of Plant Physiology and Plant Molecular Biology* **47**: 377–403
- Kaiser W. 1987. Effects of water deficit on photosynthesis capacity. *Physiologia Plantarum* **71**: 142-149.

- Kane H., Wilkin J., Portis A., Andrews T. 1998. Potent inhibition of ribulose-biphosphate carboxylase by an oxidized impurity in ribulose-1,5-biphosphate. *Plant Physiology* **177**: 1059-1069.
- Krauss S., Zhang C., Lowell B. 2005. The mitochondrial uncoupling-protein homologues. *Nature Reviews Molecular Cell Biology* **6**, 248–261.
- Krömer, S. 1995. Respiration during photosynthesis. *Annual Review of Plants Physiology and Plant Molecular Biology* **46**: 45–70.
- Lal A., Ku M., Edwards G. 1996. Analysis of inhibition of photosynthesis of photosynthesis due to water stress in the C3 species *Hordeum vulgare* and *Vicia Faba*: electron transport, CO₂ fixation and carboxylation capacity. *Photosynthesis Research* **49**: 57-69.
- Lambers H. 1982. Cyanide-resistant respiration: a non-phosphorylating electron transport pathway acting as an energy overflow. *Physiologia Plantarum* **44**: 478-485.
- Lambers H., Chapin III F., Pons T. 1998. *Plant physiological Ecology*. Springer pp. 154-209.
- Lawlor D., Cornic G. 2002. Photosynthetic carbon assimilation and associated metabolism in relation to water deficit in higher plants. *Plant, Cell and Environment* **25**: 275-294.
- Lawlor D., Tezara W. 2009. Causes of decreased photosynthetic rate and metabolic capacity in water-deficient leaf cells: a critical evaluation of mechanisms and integration of processes. *Annals of Botany* **103**: 561-579.
- Lichtenthaler H., 1987. Chlorophylls and carotenoids: pigments of photosynthetic biomembranes. *Methods in Enzymology* **148**: 350-382.
- Long S., Bernacchi C. 2003. Gas exchange measurements, what can they tell us about the underlying limitations to photosynthesis? Procedures and sources of error. *Journal of Experimental Botony* **54**: 2393-2401.
- Long S.P., Humphries S, Falkowski P.G. 1994. Photoinhibition of photosynthesis in nature. *Annual Reviews in Plant Physiology and Plant Molecular Biology* **45**: 633-662.
- Maia I., Benedetti C., Leite A., Turcinelli S., Vercesi A., Arruda P. 1998. AtPumP: an Arabidopsis gene encoding a plant uncoupling mitochondrial protein. *Federation of European Biochemical Societies Letters* **429**: 403-6.

Maroco J., Rodrigues M., Lopes C., Chaves M. 2002. Limitations to leaf photosynthesis in grapevine under drought – metabolic and modelling approaches. *Functional Plant Biology* **29**: 1-9.

Marques da Silva J., Bernardes da Silva A., Pádua M. 2007. Modulated chlorophyll a fluorescence: a tool for teaching photosynthesis. *Journal of Biological Education* **41**: 178-183.

Matos A.R., Mendes A.T., Scotti-Campos P., Arrabaça J.D. 2009. Study of the effects of salicylic acid on soybean mitochondrial lipids and respiratory properties using the alternative oxidase as a stress-reporter protein. *Physiologia Plantarum* (in press).

Maxwell D., Wang Y., McIntosh L. 1999. The Alternative Oxidase lowers mitochondrial reactive oxygen production in plant cells. *Proceedings of the National Academy of Sciences* **96**: 8271–8276.

Meinke D., Cherry J., Dean C., Rounsley S., Koornneef M. 1998. *Arabidopsis thaliana*: a model plant for genome analysis. *Science* **282**: 662-682.

Meyer S., Genty B. 1999. Heterogeneous inhibition of photosynthesis over the leaf surface of *Rosa rubiginosa* L. during water stress and abscisic acid treatment: induction of a metabolic component by limitation of CO₂ diffusion. *Planta* **210**: 126-131.

Moreno J., Martin R., Castresana C. 2005. Arabidopsis SHMT1, a serine hydroxymethyltransferase that functions in the photorespiratory pathway influences resistance to biotic and abiotic stress. *The Plant Journal* **41**, 451–463.

Niyogi K. 2000. Safety valves for photosynthesis. *Current Opinions in Plant Biology* **3**: 455–460.

Noctor, G., De Paepe, R., Foyer, C. 2007. Mitochondrial redox biology and homeostasis in plants. *Trends in Plant Science* **12**: 125–134.

Noguchi K., Yoshida K. 2008. Interaction between photosynthesis and respiration in illuminated leaves. *Mitochondrion* **8**:87–99.

Nunes C., Araújo S., Marques da Silva J., Feveireiro M., Bernardes da Silva A. 2008. Physiological responses of the legume model *Medicago truncatula* cv. Jemalong to water deficit. *Environmental and Experimental Botany* **63**: 289–296.

Nunes-Nesi A., Sulpice R., Gibon Y., Fernie A. 2008. The enigmatic contribution of mitochondrial function in photosynthesis. *Journal of Experimental Botany* **59**: 1675-1684.

Oliver D.J., 1994. The glycine decarboxylase complex from plant mitochondria. *Annual Review of Plants Physiology and Plant Molecular Biology* **45**: 323–337.

Ort D.R. 2001. When there is too much light. *Plant Physiology* **125**: 29-32

Padmasree K., Padmavathi L., Raghavendra A. 2002. Essentiality of Mitochondrial Oxidative Metabolism for Photosynthesis: Optimization of Carbon Assimilation and Protection Against Photoinhibition. *Critical Reviews in Biochemistry and Molecular Biology* **37**: 71-119

Parry M., Androlojc P., Shanhnaz K., Lea P., Keys A. 2002. Rubisco activity: effect of drought stress. *Annals of botany* **89**: 833-839.

Plaxton, W., Podestá F. 2006. The functional organization and control of plant respiration. *Critical Reviews in Plant Sciences* **25**: 159–198.

Poulson M., Regina M., Boeger T., Donahue R. 2006. Response of photosynthesis to high light and drought for *Arabidopsis thaliana* grown under a UV-B enhanced light regime. *Photosynthesis Research* **90**: 79–90.

Powles S.B. 1984. Photoinhibition of photosynthesis induced by visible light. *Annual Review of Plant Physiology* **35**: 15-44

Ristic Z., Cass D. 1991. Chloroplast structure after water shortage and high temperature in two lines of *Zea mays* L. that differ in drought resistance. *Botanical Gazette* **152**: 186-194.

Seki M., Narusaka M., Ishida J., Nanjo T., Fujita M., Oono Y., Kamiya A., Nakajima M., Enju A., Sakurai T., Satou M., Akiyama K., Taji T., Yamaguchi-Shinozaki K., Carninci P., Kawai J., Hayashizaki Y., Shinozaki K. 2002. Monitoring the expression profiles of 7000 *Arabidopsis* genes under drought, cold and high-salinity stresses using a full-length cDNA microarray. *The Plant Journal* **31**: 279-292.

Sharkey T., Seeman J. 1988. Mild water stress effects on carbon reduction cycle intermediates ribulose biphosphate carboxylase activity, and special homogeneity of photosynthesis in intact leaves. *Plant Physiology* **89**: 1060-1065.

Sharkey T., Bernacchi C., Farquhar G, Singsaas E. 2007. Fitting photosynthetic carbon dioxide response curves for C3 leaves. *Plant, Cell and Environment* **30**: 1035-1040.

Siedow J., Umbach A. 2000. The mitochondrial cyanide-resistant oxidase: structural conservation amid regulatory diversity. *Biochimica et Biophysica Acta* **1459**: 432-439.

Simons B., Millenaar F., Mulder L., Van Loon L., Lambers H. 1999. Enhanced expression and activation of the Alternative Oxidase during infection of *Arabidopsis* with *Pseudomonas syringae pv tomato*. *Plant Physiology* **120**: 529–538.

Shinozaki K., Yamaguchi-Shinozaki K. 1997. Gene expression and signal transduction in water-stress response. *Plant Physiology* **115**: 327-334.

Smith A., Ratcliffe R., Sweetlove L. 2004. Activation and function of mitochondrial uncoupling protein in plants. *The Journal of Biological Chemistry* **50**: 51944–51952.

Strodtkötter I., Padmasree K., Dinakar C., Speth B., Niazi P., Wojtera J., Voss I., Thi Do P., Nunes-Nesi A., Fernie A., Linke V., Raghavendra A., Scheibe R. 2009. Induction of the AOX1d isoform of alternative oxidase in *A. thaliana* t-dna insertion lines lacking isoform AOX1a is insufficient to optimize photosynthesis when treated with antimycin A. *Molecular Plant* **2**: 284–297

Sweetlove L., Lytovchenko A., Morgan M., Nunes-Nesi A., Taylor N., Baxter C., Eickmeier I, Fernie A. 2006. Mitochondrial uncoupling protein is required for efficient photosynthesis. *Proceedings of the National Academy of Sciences* **103**: 19587–19592.

Tabata S., Kaneko T., Nakamura Y., Kotani H., Kato T., Asamizu E., Miyajima N., Sasamoto S., Kimura T., Hosouchi T., Kawashima K., Kohara M., Matsumoto M., Matsuno A., Muraki A., Nakayama S., Nakazaki N., Naruo K., Okumura S., Shinpo S., Takeuchi C., Wada T., Watanabe A., Yamada M., Yasuda M., Sato S., de la Bastide M., Huang E., Spiegel L., Gnoj L., O’Shaughnessy A., Preston R., Habermann K., Murray J., Johnson D., Rohlffing T., Nelson J., Stoneking T., Pepin K., Spieth J., Sekhon M., Armstrong J., Becker M., Belter E., Cordum H., Cordes M., Courtney L., Courtney W., Dante M., Du H., Edwards J., Fryman J., Haakensen B., Lamar E., Latreille P., Leonard S., Meyer R., Mulvaney E., Ozersky P., Riley A., Strowmatt C., Wagner-McPherson C., Wollam A., Yoakum M., Bell M., Dedhia N., Parnell L., Shah R., Rodriguez M, See LH, Vil D, Baker J, Kirchoff K, Toth K, King L, Bahret A, Miller B, Marra M, Martienssen R., McCombie R., Wilson K., Murphy G., Bancroft I., Volckaert G., Wambutt R., Dusterhöft A., Stiekema W., Pohl T., Entian K., Terry N., Hartley N., Bent E., Johnson S., Langham S., McCullagh B., Robben J., Grymonprez B., Zimmermann W., Ramsperger U., Wedler H., Balke K., Wedler E., Peters S., van Staveren M., Dirkse W., Mooijman P., Lankhorst R., Weitzenegger T., Bothe G., Rose M., Hauf J., Berneiser S., Hempel S., Feldpausch M., Lamberth S., Villarreal R., Gielen J, Ardiles W., Bents O., Lemcke K., Kolesov G., Mayer K., Rudd S., Schoof H., Schueller C., Zaccaria P., Mewes H., Bevan M., Fransz P. 2000. Sequence and analysis of chromosome 5 of the plant *Arabidopsis thaliana*. *Nature* **408**: 823-826.

Tezara W., Mitchell V., Driscoll S., Lawlor D. 1999. Water stress inhibits plant photosynthesis by decreasing coupling factor and ATP. *Nature* **401**: 914–917.

Umbach A., Fiorani F., Siedow J. 2005. Characterization of transformed *Arabidopsis* with altered Alternative Oxidase levels and analysis of effects on reactive oxygen species in tissue. *Plant Physiology* **139**: 1806–1820.

Vanlerberghe G., McIntosh L. 1997. Alternative Oxidase: from gene to function. *Annual Review of Plant Physiology and Plant Molecular Biology* **48**: 703-734.

Voll L.M., Jamai A, Renne´ P, Voll H, McClung C.R., Weber A.P. 2006. The photorespiratory *Arabidopsis* shm1 mutant is deficient in SHM1. *Plant Physiology* **140**: 59–66.

Von Caemmerer S. 2000. Biochemical models of leaf photosynthesis. CSIRO Publishing, Collingwood, Australia.

Watanabe C., Hachiya T., Terashima I., Noguchi K. 2008. The lack of alternative oxidase at low temperature leads to a disruption of the balance in carbon and nitrogen metabolism, and to an up-regulation of antioxidant defense systems in *Arabidopsis thaliana* leaves. *Plant, Cell and Environment* **31**: 1190-1202.

7. Attachments

Equations:

Fig. 1

A

$$\text{Col-0} - Y = 0,415X - 12,0$$

B

$$\text{Col-0} - Y = 0,786 + 40,52X - 20,47X^2$$

C

$$\text{Col-0} - Y = 30,8X + 28,1$$

Fig. 3

$$\text{Col-0} - Y = 3,143X + 239,0$$

$$\text{AS-AOX1a} - Y = 5,28X + 149,3$$

Fig. 4

A

$$\text{Col-0} - Y = 1,951 + 0,045X - 0,0003X^2$$

$$\text{AS-AOX1a} - Y = -2,003 + 0,037X - 0,0002X^2$$

B

$$\text{Col-0} - Y = -2,594 + 0,066X - 0,0005X^2$$

$$\text{AS-AOX1a} - Y = -2,231 + 0,045X - 0,00028X^2$$

Fig. 5

$$\text{Col-0} - Y = 0,006X - 0,125$$

$$\text{AS-AOX1a} - Y = 0,02X - 0,749$$

Fig. 6

A

$$\text{Col-0} - Y = 1,392X - 14,98$$

$$\text{AS-AOX1a} - Y = 0,418X + 39,68$$

B

$$\text{Col-0} - Y = 1,685X + 39,79$$

$$\text{AS-AOX1a} - Y = 0,576X + 110,7$$

C

$$\text{Col-0} - Y = 0,147X + 3,18$$

$$\text{AS-AOX1a} - Y = 0,03X + 11,23$$

Fig. 7

A

$$\text{Col-0} - Y = 0,415X - 12,09$$

$$\text{AS-AOX1a} - Y = 0,325X - 8,0$$

B

$$\text{Col-0} - Y = 0,072X + 0,045$$

$$\text{AS-AOX1a} - Y = -12,3 + 0,507X - 0,004X^2$$

C

$$\text{Col-0} - Y = 0,019 + 0,016X - 0,0002X^2$$

$$\text{AS-AOX1a} - Y = -0,003X + 0,521$$

Fig. 8

A

$$\text{Col-0} - Y = 0,002X - 0,081$$

$$\text{AS-AOX1a} - Y = 0,002X - 0,065$$

B

$$\text{Col-0} - Y = 0,61X - 19,37$$

$$\text{AS-AOX1a} - Y = 0,348X - 3,347$$

C

$$\text{Col-0} - Y = -3,325X + 261,0$$

$$\text{AS-AOX1a} - Y = -1,929X + 145,5$$

Fig. 9

A

$$\text{Col-0} - Y = -0,259X + 158,6$$

$$\text{AS-AOX1a} - Y = 242,1 - 4,721X + 0,039X^2$$

B

$$\text{Col-0} - Y = -1,051X + 774,6$$

$$\text{AS-AOX1a} - Y = -2,743X + 821,72$$

C

$$\text{Col-0} - Y = -0,0006X + 0,791$$

$$\text{AS-AOX1a} - Y = 0,722 + 0,004X - 4,086e^{-5}X^2$$

Fig. 10

A

$$\text{Col-0} - Y = 0,043X + 51,30$$

$$\text{AS-AOX1a} - Y = 28,66 + 1,089X - 0,01X^2$$

B

$$\text{Col-0} - Y = 0,414X + 88,44$$

$$\text{ÁS-AOX1a} - Y = 3,19 + 4,24X - 0,04X^2$$

C

$$\text{Col-0} - Y = 0,001X + 0,71$$

$$\text{AS-AOX1a} - Y = 0,0007X + 0,728$$

D

$$\text{Col-0} - Y = 0,002X + 0,617$$

$$\text{AS-AOX1a} - Y = 0,471 + 0,008X - 6,688e^{-5}X^2$$

E

$$\text{Col-0} - Y = -0,0001X + 0,806$$

$$\text{AS-AOX1a} - Y = -0,0005X + 0,845$$

F

$$\text{Col-0} - Y = 0,001X + 0,577$$

$$\text{AS-AOX1a} - Y = 0,622 + 0,005X - 4,64e^{-5}X^2$$

G

$$\text{Col-0} - Y = 0,0008X + 0,339$$

$$\text{AS-AOX1a} - Y = 0,153 + 0,011X - 0,0001X^2$$

H

$$\text{Col-0} - Y = -0,003X + 0,970$$

$$\text{AS-AOX1a} - Y = -0,009X + 1,303$$

Fig. 11

A

$$\text{Col-0} - Y = -1,65X + 843$$

$$\text{AS-AOX1a} - Y = 9,315X + 303$$

B

$$\text{Col-0} - Y = -0,954X + 405,5$$

$$\text{AS-AOX1a} - Y = 2,576X + 125,6$$

C

$$\text{Col-0} - Y = -2,65X + 1253$$

$$\text{AS-AOX1a} - Y = 11,89X + 428,8$$

H

Col-0 – $Y = -0,152X + 107,8$

AS-AOX1a – $Y = 1,5X + 63,8$